

CHARACTERIZATION, PHYSICAL PROPERTIES AND COMMERCIAL
VIABILITY OF BLENDED CEMENTS WITH HIGH
VOLUME INTERGROUND LIMESTONE

by

Ashley Russell Kotwal, M.S.T.

A dissertation submitted to the Graduate Council of
Texas State University in partial fulfillment
of the requirements for the degree of
Doctor of Philosophy
with a Major in Materials Science, Engineering & Commercialization
December 2015

Committee Members:

Thomas Myers, Chair

John Schemmel

Vedaraman Sriraman

Clois Powell

Craig Hanks

COPYRIGHT

by

Ashley Russell Kotwal

2015

FAIR USE AND AUTHOR'S PERMISSION STATEMENT

Fair Use

This work is protected by the Copyright Laws of the United States (Public Law 94-553, section 107). Consistent with fair use as defined in the Copyright Laws, brief quotations from this material are allowed with proper acknowledgement. Use of this material for financial gain without the author's express written permission is not allowed.

Duplication Permission

As the copyright holder of this work I, Ashley Russell Kotwal, refuse permission to copy in excess of the "Fair Use" exemption without my written permission.

DEDICATION

For Hillary Kate

ACKNOWLEDGEMENTS

It is with great appreciation that I acknowledge my dissertation committee chair, Dr. Thomas Myers, for his unwavering support and contribution to the betterment of my education. I offer him my sincerest gratitude for his encouragement and guidance throughout all the endeavors that I pursued as a doctoral student.

I would like to thank my dissertation committee members, Dr. John Schemmel, Dr. Vedaraman Sriraman, Dr. Clois Powell and Dr. Craig Hanks, whose enthusiasm and dedication provided a major driving force for me to strive for excellence and integrity in my work.

This study would not have been possible without the resources and support provided by Capitol Aggregates, Baker Concrete Construction, William Coker and the Graduate College. As a direct result of their contribution, I was able to improve the design of my experiments, adequately interpret the results and explain plausible implications.

I am extremely grateful for the training and assistance provided by Shane Arabie, Ted Cera, Eric Schires, Justin Dickey, Cody Young, Andres Sanchez, Declan Ward and many other staff members and students in the College of Science and Engineering. The sharing of their knowledge and time was invaluable to the successful completion of this research project.

Finally, the role of my family can hardly be overstated. I would like to thank them for thirty years of unconditional faith, hope and love.

TABLE OF CONTENTS

	Page
ACKNOWLEDGEMENTS.....	v
LIST OF TABLES.....	viii
LIST OF FIGURES.....	ix
ABSTRACT.....	xii
CHAPTER	
I. INTRODUCTION.....	1
1.1 Overview.....	1
1.2 Concrete Materials.....	3
1.3 Research Significance.....	5
1.4 Research Objectives.....	6
1.5 Scope of Work.....	6
1.6 Analytical Techniques.....	8
1.7 Assumptions.....	8
1.8 Limitations.....	9
1.9 Delimitations.....	9
II. CEMENT.....	10
2.1 Overview.....	10
2.2 Blaine Fineness.....	10
2.3 Particle Size Distribution.....	13
2.4 X-Ray Diffraction.....	15
2.5 X-Ray Fluorescence.....	20
2.6 Specific Gravity.....	24
III. AGGREGATE.....	25
3.1 Overview.....	25
3.2 Sieve Analysis.....	25
3.3 Specific Gravity and Absorption.....	27

IV. MORTAR	30
4.1 Overview	30
4.2 Flow	30
4.3 Isothermal Calorimetry	32
4.4 Setting Time.....	34
4.5 Compressive Strength.....	37
4.6 Drying Shrinkage	40
4.7 Sulfate Expansion	41
V. CONCRETE.....	43
5.1 Overview	43
5.2 Fresh Concrete Properties.....	44
5.3 Petrography	48
5.4 Compressive Strength	51
5.5 Splitting Tensile Strength	53
5.6 Flexural Strength.....	56
5.7 Modulus of Elasticity.....	58
5.8 Freeze-Thaw Resistance	61
VI. COMMERCIAL VIABILITY	68
6.1 Overview.....	68
6.2 Market Analysis	69
6.3 Competitor Analysis	71
6.4 Case Studies	72
6.5 Life Cycle Assessment.....	73
VII. DISCUSSION	77
7.1 Summary	77
7.2 Conclusions.....	77
7.3 Recommendations.....	79
7.4 Future Research	80
LITERATURE CITED	81

LIST OF TABLES

Table	Page
2.1 Cement Types	10
2.2 Blaine Fineness of Cement	12
2.3 Oxide Compounds of Cement.....	23
2.4 Primary Phases of Cement	23
2.5 Specific Gravity of Cement	24
3.1 Specific Gravity and Absorption of Aggregate	29
4.1 Flow of Mortar	31
4.2 Specified Compressive Strength of Mortar.....	37
4.3 Compressive Strength of Mortar.....	39
5.1 Volumetric Concrete Mix Design.....	44
5.2 Fresh Concrete Properties	47
5.3 Splitting Tensile Strength of Concrete.....	55
5.4 Modulus of Rupture of Concrete	57
5.5 Modulus of Elasticity of Concrete	61
5.6 Durability Factor of Concrete	67
6.1 Cement Plant Locations in Texas	69
6.2 Historical Use of Limestone in Cement.....	70
6.3 Energy Consumption and CO ₂ Emissions of Cement Manufacturing.....	75
6.4 Energy Consumption and CO ₂ Emissions of Blended Cement Manufacturing	75

LIST OF FIGURES

Figure	Page
1.1 Texas Cement Capacity and Projected Demand.....	1
1.2 Cement Manufacturing Plant.....	3
2.1 Blaine Air Permeability Apparatus.....	12
2.2 Malvern Mastersizer Particle Size Analyzer.....	14
2.3 Particle Size Distribution of Cement.....	15
2.4 Diffraction of X-Rays by Crystal Planes.....	16
2.5 Crystalline Structure of Alite.....	17
2.6 X-Ray Diffraction of Cement and Primary Phases.....	18
2.7 Bruker D8 Advanced Eco A25 Diffractometer.....	19
2.8 X-Ray Diffraction of Cement.....	20
2.9 Panalytical Axios X-Ray Fluorescence Spectrometer.....	22
3.1 Aggregate Gradations.....	26
3.2 Sieve Analysis of Aggregate.....	27
3.3 Moisture Conditions of Aggregate.....	27
4.1 Calmetrix I-Cal 8000 Isothermal Calorimeter.....	33
4.2 Heat Generation of Mortar.....	34
4.3 Acme Mortar Penetrometer.....	36
4.4 Setting Time of Mortar.....	36
4.5 Setup for Compressing Mortar.....	38

4.6 Compressive Strength of Mortar.....	39
4.7 Length Comparator and Mortar Prisms	40
4.8 Drying Shrinkage of Mortar.....	41
5.1 Crown C6 Concrete Drum Mixer	43
5.2 Slump Cone, Thermometer, Air Meter and Associated Tools.....	46
5.3 Scanning Electron Microscope Column and Control Console	49
5.4 JEOL JSM-6010Plus/LA Analytical Scanning Electron Microscope	50
5.5 Micrograph of Concrete Matrix	50
5.6 Setup for Compressing Concrete	52
5.7 Compressive Strength of Concrete	52
5.8 Correlation of Mortar and Concrete Compressive Strength	53
5.9 Setup for Splitting Concrete.....	54
5.10 Correlation of Splitting Tensile Strength and Compressive Strength.....	55
5.11 Setup for Flexing Concrete	57
5.12 Correlation of Modulus of Rupture and Compressive Strength	58
5.13 Stress-Strain Relationship of Concrete	59
5.14 Setup for Elastically Deforming Concrete	61
5.15 Forced Resonance Test Schematic.....	63
5.16 Freeze-Thaw Weathering Regions.....	64
5.17 Setup for Freezing and Thawing Concrete	65
5.18 Setup for Resonating Concrete	65

5.19 Mass Change of Concrete	66
5.20 Deterioration of Concrete Beams from Freezing and Thawing.....	67
6.1 Geologic Map of Texas.....	68
6.2 Cement Types Produced in Europe.....	70
6.3 Overview of the Gotthard Base Tunnel Project Site.....	72
6.4 Process Flow Diagram of Cement Manufacturing.....	74
6.5 Energy Consumption and CO ₂ Emissions of Blended Cement Manufacturing	76

ABSTRACT

The production of cement is one of the largest sources of energy consumption and carbon dioxide emissions in the world. Although cement is critical to the development of most infrastructure, regulations and permitting make it extremely cumbersome to increase production capacity. Consequently, the investigation of cement replacement in concrete mixtures is considered to be of commercial significance in the construction industry. Intergrinding limestone with clinker enables cement manufacturers to increase overall production volume while decreasing energy consumption and carbon dioxide emissions. To take advantage of these benefits, this study investigated the production and application of blended cements with high volume interground limestone. The characteristics of the materials were evaluated as well as their effect on the physical properties of mortar and concrete to determine their viability. A life cycle assessment was also performed to support commercialization of the blended cements.

I. INTRODUCTION

1.1 Overview

Urban land in the United States is projected to double by 2030 (Seto et al., 2012). Many of the structures and pavements built in the expanding urban environment will be constructed with concrete. Consequently, concrete will continue to be the most widely used construction material and the second most consumed resource in the world. Thus, the demand for the basic constituents of concrete will also grow (Atakan et al., 2014).

Texas is the largest producer and consumer of cement in the United States (Prusinski, 2014). As shown in Figure 1.1, projections for the demand of cement in Texas quickly outpace production and import capacity. Including announced production expansions, it is estimated that native production capacity and foreign import capacity will be exceeded as early as 2017 and 2024, respectively.

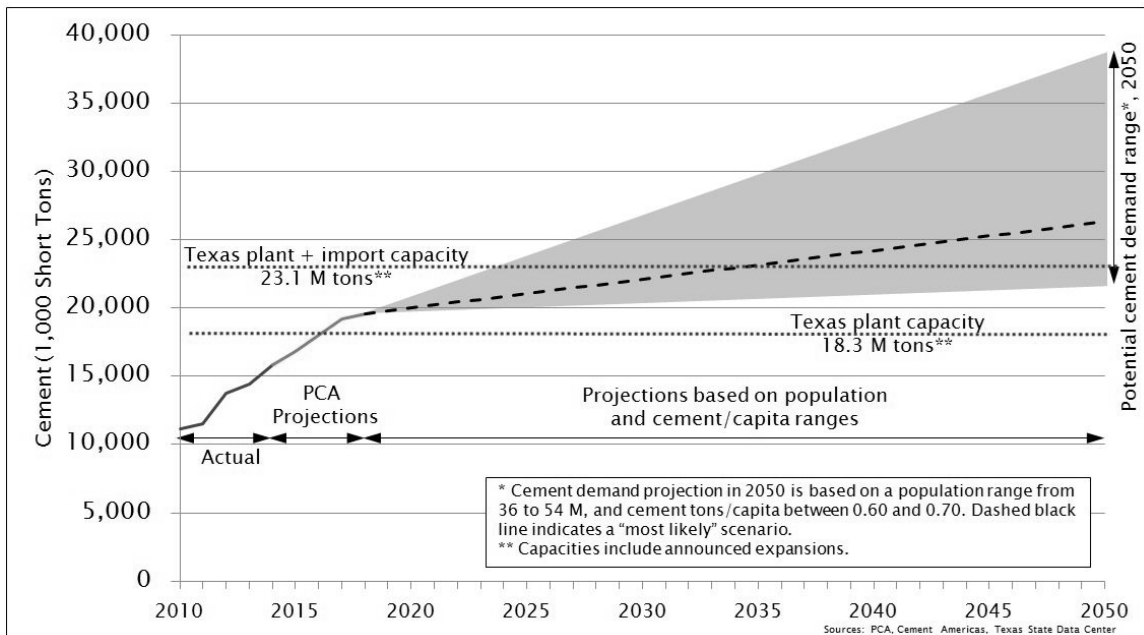


Figure 1.1 Texas Cement Capacity and Projected Demand (Prusinski, 2014).

To increase the overall production volume of cement while reducing energy consumption and hazardous emissions, manufacturers produce blended cements by combining ordinary portland cement with supplementary cementitious materials. An alternative approach is to produce portland limestone cement conforming to ASTM C595 (2013). This material is manufactured by blending ordinary cement with limestone as a mineral admixture. Currently, limestone content is limited to 15% by mass. However, to produce a more sustainable material, it will be necessary to blend larger amounts of the mineral admixture with ordinary cement.

It is commonly known that manufacturing cement consumes large quantities of energy. Figure 1.2 illustrates an example of a cement manufacturing plant. Although layouts and equipment differ at every plant, the operational steps of the modern production process are generally the same. Raw material sources of calcium carbonate, silica, alumina and iron are quarried and milled into a fine powder. These materials are then fed into a preheater tower and rotary kiln where they undergo an endothermic reaction called calcination. During the calcination process, calcium carbonate is converted to calcium oxide and carbon dioxide. Silicates combine with calcium oxide to form round crystals known as belite or dicalcium silicate. The subsequent reaction between belite and calcium oxide forms angular crystals known as alite or tricalcium silicate. Agglomeration of these particles forms clinker nodules as the rotary kiln temperature reaches approximately 2,500°F. When the clinker cools, alumina and iron contribute to the formation of tricalcium aluminate and tetracalcium aluminoferrite phases within the nodules. Finally, clinker is combined with a small amount of calcium sulfate and ground into a fine powder. It is in the final milling step that an opportunity is

presented to intergrind limestone to produce portland limestone cement. Thus, a greater volume of cement is produced with little to no increase in energy consumption.

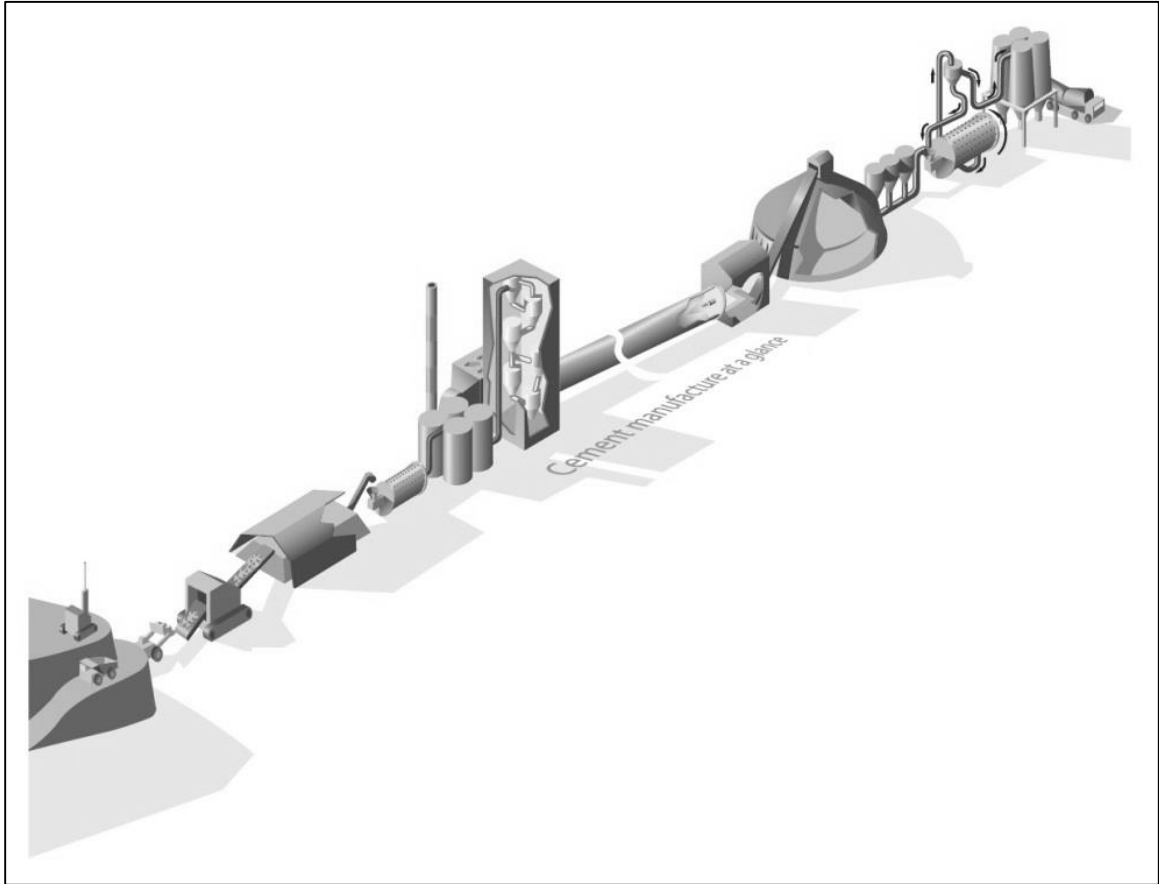


Figure 1.2 Cement Manufacturing Plant (WBCSD, 2012).

1.2 Concrete Materials

Concrete is a composite material containing a mixture of cement, water, fine aggregate and coarse aggregate. For many test procedures and industrial applications, the coarse aggregate is excluded to make mortar. In addition to their basic constituents, concrete and mortar mixtures often contain chemical and mineral admixtures to achieve a higher level of performance and sustainability. The following subsections provide an overview of the constituent materials.

1.2.1 Cement

Cement is the principal component in concrete which exothermically reacts with water to bind the fine and coarse aggregates. The hydration of alite and belite form calcium silicate hydrate, the primary compound responsible for strength and durability. Other reaction products include calcium hydroxide, ettringite, monosulfoaluminate, calcium aluminate hydrate and calcium aluminoferrite hydrate. These compounds are embedded in the matrix but do not contribute significantly to strength (Taylor, 1997).

Blended cements reduce the carbon footprint of concrete by using less clinker to produce a given volume. These cements are produced either by intergrinding mineral admixtures with clinker at the manufacturing plant or by blending admixtures with cement powder after production. Many mineral admixtures are byproducts of industrial processes, such as fly ash, slag and silica fume. These materials are referred to as pozzolans and chemically react with calcium hydroxide to form cementitious compounds (Detwiler et al., 1996).

Due to the growing need to increase cement production capacity, limestone is currently being investigated for its potential use in blended cements. Limestone is a sedimentary rock that is primarily composed of calcium carbonate. Previous research has indicated that this mineral admixture is mostly inert and acts as a filler. Intergrinding limestone with clinker has been shown to produce cement with a wider particle size distribution. Since limestone is softer than clinker, portland limestone cement is often finer and has higher surface area. These characteristics impact water demand, packing density and strength (Tennis et al., 2011).

1.2.2 Aggregate

Fine and coarse aggregates typically account for 60% to 75% of the total concrete volume or 70% to 85% of its mass. Fine aggregate has a maximum nominal particle size of about 0.2 in. The particle size of coarse aggregate generally ranges from 0.2 in. up to 1.5 in., although larger aggregate may be used in specialized applications. Aggregates are obtained from natural and manufactured sources. They are produced with a continuous gradation to improve particle packing and maximize the efficiency of the cement (Kosmatka et al., 2003).

1.2.3 Chemical Admixtures

Enhanced workability, finishability, strength, durability, permeability and wear resistance of concrete can be obtained through the use of chemical admixtures. For example, when the desired effect is improved freeze-thaw durability, an air-entraining admixture is often used. A small amount of air naturally becomes entrapped in concrete during the mixing process. Air-entraining admixtures introduce an additional network of microscopic air voids that allow water to expand and contract during freeze-thaw cycles to prevent substantial deterioration from hydraulic pressure (Whiting & Nagi, 1998).

1.3 Research Significance

Previous studies of portland limestone cement have focused mainly on cement containing up to 15% limestone. Furthermore, limited research has been conducted on the durability of portland limestone cement and its interaction with fly ash. Original contribution to the scientific literature was made in this study to fill gaps in the existing body of knowledge regarding the characteristics and physical properties of blended

cement with limestone content up to 25%. A ternary blend with fly ash was also investigated, as it is the most widely used supplementary cementitious material.

1.4 Research Objectives

The present study analyzed the effect of interground limestone on the characteristics of blended cements as well as the properties of mortar and concrete manufactured with the blended cements. The purpose was to develop technical data and practical information that will enable the construction industry to utilize portland limestone cement as an alternative to ordinary portland cement. An objective of this study was to determine if acceptable physical properties of mortar and concrete could be obtained by using cement with up to 25% limestone. The commercial viability and potential applications of portland limestone cement were also investigated.

1.5 Scope of Work

A cement manufacturer was consulted to assist with the design of the experimental program, including the selection of constituent materials, development of mixture proportions and identification of independent and dependent variables. All physical tests were completed in accordance with applicable ASTM International standards or recommended procedures of the cement manufacturer.

The experimental program began by determining the characteristics of the constituent materials. The following tests were performed for this portion of the study:

- Cement
 - Blaine Fineness
 - Particle Size Distribution
 - X-Ray Diffraction
 - X-Ray Fluorescence
 - Specific Gravity

- Aggregates
 - Sieve Analysis
 - Specific Gravity
 - Absorption

The ability to place fresh concrete is dependent on its hardening behavior and compaction requirements. Once the concrete has hardened, compressive strength is commonly considered to be its most important mechanical property. Although, in some cases, its elasticity or durability may be more critical. The following tests were performed to provide a thorough understanding of the properties of mortar and concrete in both fresh and hardened states:

- Mortar
 - Flow
 - Isothermal Calorimetry
 - Setting Time
 - Compressive Strength
 - Drying Shrinkage
 - Sulfate Attack
- Concrete
 - Slump
 - Temperature
 - Density
 - Yield
 - Air Content
 - Petrography
 - Compressive Strength
 - Splitting Tensile Strength
 - Flexural Strength
 - Modulus of Elasticity
 - Freeze-Thaw Resistance

Sustainable cements are formulated and manufactured to minimize the total environmental impact during their entire life cycle. The replacement of high levels of cement with limestone has the potential to further decrease this impact. To evaluate the influence of this technology, a life cycle assessment was conducted by compiling an

inventory of energy and emission elements related to the cement manufacturing process. The results were interpreted to ascertain the environmental implications of producing blended cements with high volume interground limestone.

1.6 Analytical Techniques

Portions of the data were subjected to an analysis of variance to substantiate if the measured variation was statistically significant. This inferential statistical method established the magnitude of the total variation in the results and distinguished the random variation from the contribution of each variable. A conventional level of significance ($p < 0.05$) was used for the analysis. To determine if there was a significant correlation ($R^2 > 0.95$) between various measurements, regression analysis was performed as well.

1.7 Assumptions

Slight variations in particle size and chemical composition may exist within any given sample of material. This research was based on the assumption that all constituent materials were homogeneous with respect to their characteristics. Precautions were taken in accordance with standard testing procedures to ensure that representative samples of all materials were obtained.

The Bogue equations in the ASTM C150 (2012) standard specification for portland cement were used to quantify the primary cement phases. These calculations assumed that the compounds were crystalline and that there were no impurity oxides. Additionally, all iron present was assumed to be agglomerated in the tetracalcium

aluminoferrite phase, and the remaining alumina was contained in the tricalcium aluminate. The alite and belite phases were then quantified based on the silica content.

1.8 Limitations

This study was limited by the source of the raw materials, and thus the composition of the cement and aggregates. Materials that meet ASTM specifications were used, although these are valid within a certain range and may deviate slightly when obtained from other sources.

Testing of the materials was performed in a controlled laboratory setting, thereby limiting the external validity to other environments. Results may vary based on the temperature, humidity and pressure of the environment in which the materials are used.

1.9 Delimitations

The complexity of concrete allows numerous independent variables to be manipulated in research. For the purpose of this study, it was established that the only independent variable would be the type of cement due to the large number of dependent variables being evaluated. Depending on the property being measured, boundaries were also set on the testing time and number of specimens while still following standard testing procedures and ensuring that reliable data would be obtained.

Although several considerations were made during the life cycle assessment, too many variables exist to perform a complete analysis within the scope of work of the study. The cost of material and energy was not included, as the sources vary greatly depending on the plant location. For this same reason, the effect on raw material depletion was not evaluated.

II. CEMENT

2.1 Overview

Cement performance is directly related to its constituent crystalline phases. Therefore, the use of portland limestone cement requires thorough knowledge of its characteristics, which are primarily influenced by particle size and chemical composition (Schiller & Ellerbrock, 1992).

The cement types considered in this study are shown in Table 2.1. Nominal values of interground limestone and Class F fly ash are stated by mass percentage. The blended cements were produced by intergrinding the mineral admixtures in the finish mill at a local cement plant. Type I general purpose cement was included in the testing regime as a baseline for comparison. Testing of the cements and associated outcomes are discussed in the sections which follow.

Table 2.1 Cement Types.

Cement Type	Limestone Content (% by Mass)	Class F Fly Ash Content (% by Mass)
I	5	0
IL(15)	15	0
IL(25)	25	0
IT(L15)(P25)	15	25

2.2 Blaine Fineness

2.2.1 Background

The hydration rate of cement is greatly dependent on its fineness. Typically, increased fineness corresponds with faster reactivity. For quality control and research purposes, the surface area of cement is measured with a Blaine air permeability apparatus

to provide an indication of its fineness. This test is based on the rate at which air passes through a chamber of cement under a known pressure gradient. The resulting Blaine fineness value ranges from 3000 cm²/g to 5000 cm²/g for ordinary cement. Blaine fineness is calculated in accordance with the following equation:

$$S = \frac{S_s \rho_s (b_s - \varepsilon_s) \sqrt{\eta_s} \sqrt{\varepsilon_s^3} \sqrt{T}}{\rho (b - \varepsilon) \sqrt{\eta} \sqrt{\varepsilon^3} \sqrt{T_s}}$$

where:

- S = surface area of the test sample, cm²/g
- S_s = surface area of the standard calibration sample, cm²/g
- ρ = relative density of the test sample, g/cm³
- ρ_s = relative density of the standard calibration sample, g/cm³
- b = constant value of 0.9
- b_s = constant value of 0.9
- ε = porosity ratio of the test sample
- ε_s = porosity ratio of the standard calibration sample
- η = viscosity of air at the temperature of the test sample, $\mu\text{Pa}\cdot\text{s}$
- η_s = viscosity of air at the temperature of the standard calibration sample, $\mu\text{Pa}\cdot\text{s}$
- T = measured time interval of manometer drop for the test sample, s
- T_s = measured time interval of manometer drop for the standard calibration sample, s

Caldarone (2006) and Kumar et al. (2013) studied the effect of limestone on various properties of cement. Their results indicated that intergrinding 15% limestone with clinker increased the Blaine fineness of the blended cement when compared to ordinary cement. These findings were attributed to the fact that limestone grinds more readily than clinker in the finish mill, producing a greater proportion of smaller particles. Thus, a higher surface area was measured for the material as a whole.

2.2.2 Methodology and Results

As specified in ASTM C204 (2011), the fineness of each cement type was quantified using the Blaine air permeability apparatus shown in Figure 2.1. Grinding the

cement in the finish mill resulted in the values reported in Table 2.2. With a consistent milling duration, the surface area increased as more limestone was interground with clinker, ranging from 3,760 cm²/g to 4,840 cm²/g. The ternary blend was found to have an intermediate surface area similar to Type IL(15). All measurements exceeded the minimum fineness of 2600 cm²/g specified for Type I in ASTM C150 (2012), suggesting that an increased rate of hydration could occur due to higher surface area. However, additional analysis was required as Blaine fineness does not provide an indication of the actual cement particle sizes or their chemical composition.



Figure 2.1 Blaine Air Permeability Apparatus.

Table 2.2 Blaine Fineness of Cement.

Cement Type	Blaine Fineness (cm²/g)
I	3,760
IL(15)	4,390
IL(25)	4,840
IT(L15)(P25)	4,170

2.3 Particle Size Distribution

2.3.1 Background

Measuring the particle size distribution provides a more detailed analysis in order to obtain important insight regarding hydration behavior. A common technique used for this analysis is laser diffraction. This characterization method measures the angular variation in light intensity as it is scattered by a laser beam. Large particles scatter light at smaller angles, and small particles scatter light at larger angles relative to the laser. By analyzing the measured angular scattering intensity through a dispersed particulate sample, the particle size is expressed as a volume equivalent sphere diameter as per the Mie theory of light scattering (Malvern, 2015).

When water reacts with a cement particle, hydration products form around the outer layer. As a result, the outer layer separates the unreacted core from the surrounding water. Smaller particles tend to react more rapidly, because a thicker layer of hydration products will delay the reaction. Consequently, 1 μm particles completely react in about a day, 10 μm particles completely react within a month, and particles larger than 50 μm may never completely react (Thomas & Jennings, 2015).

In an investigation of portland limestone cement, Caldarone (2006) found that a larger volume of the finer particles consisted of limestone. It was proposed that the particle size distribution of cement containing limestone would be more uniformly graded. This proposition led to the conclusion that denser particle packing in the cement matrix resulted from intergrinding low volumes of limestone with clinker.

2.3.2 Methodology and Results

The particle size distribution of each cement type was measured with the Malvern Mastersizer particle size analyzer presented in Figure 2.2. The distribution curves in Figure 2.3 indicate that the cement particles ranged in size from about 0.1 μm to 100 μm . All cement types exhibited a primary peak at approximately 30 μm and a secondary peak at 0.35 μm . Larger volumes of fine particles were measured in cement containing higher levels of limestone. Type IL(25) also had a larger amount of coarse particles near the 100 μm end of the spectrum, thereby decreasing the volume near the 30 μm peak and creating a more even distribution compared to Type I. The distribution of the ternary blend closely resembled the Type IL(15) curve but was found to have a lower volume of fine particles near the 0.35 μm peak. Although laser diffraction provided additional insight, it was unable to distinguish the limestone and fly ash from the cement.

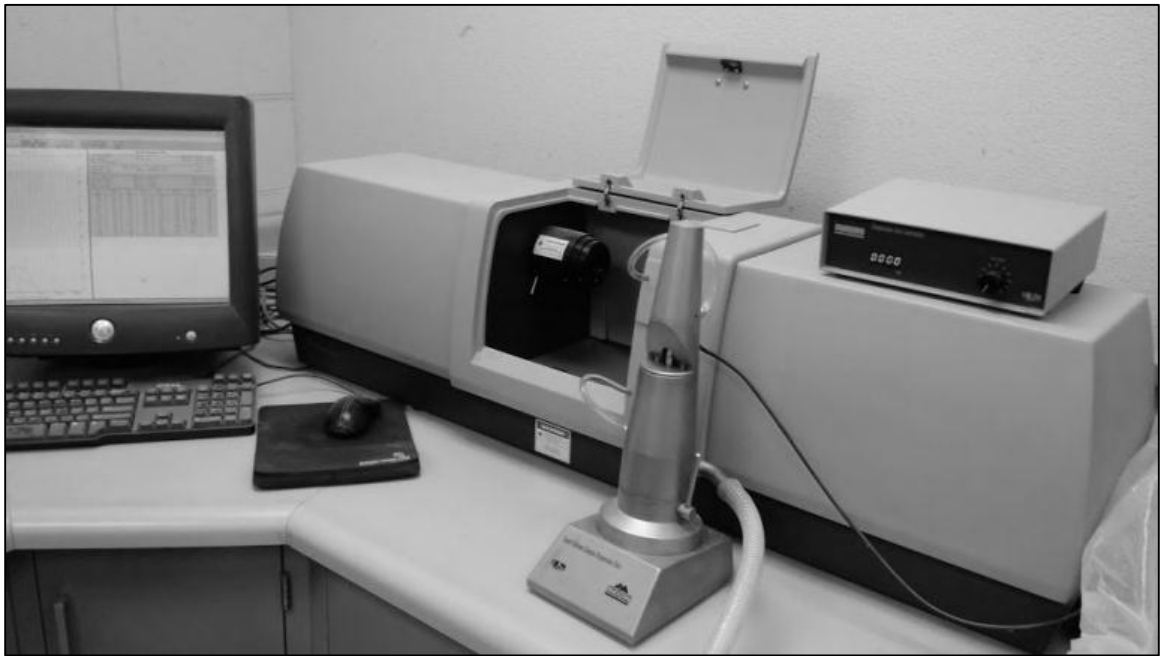


Figure 2.2 Malvern Mastersizer Particle Size Analyzer.

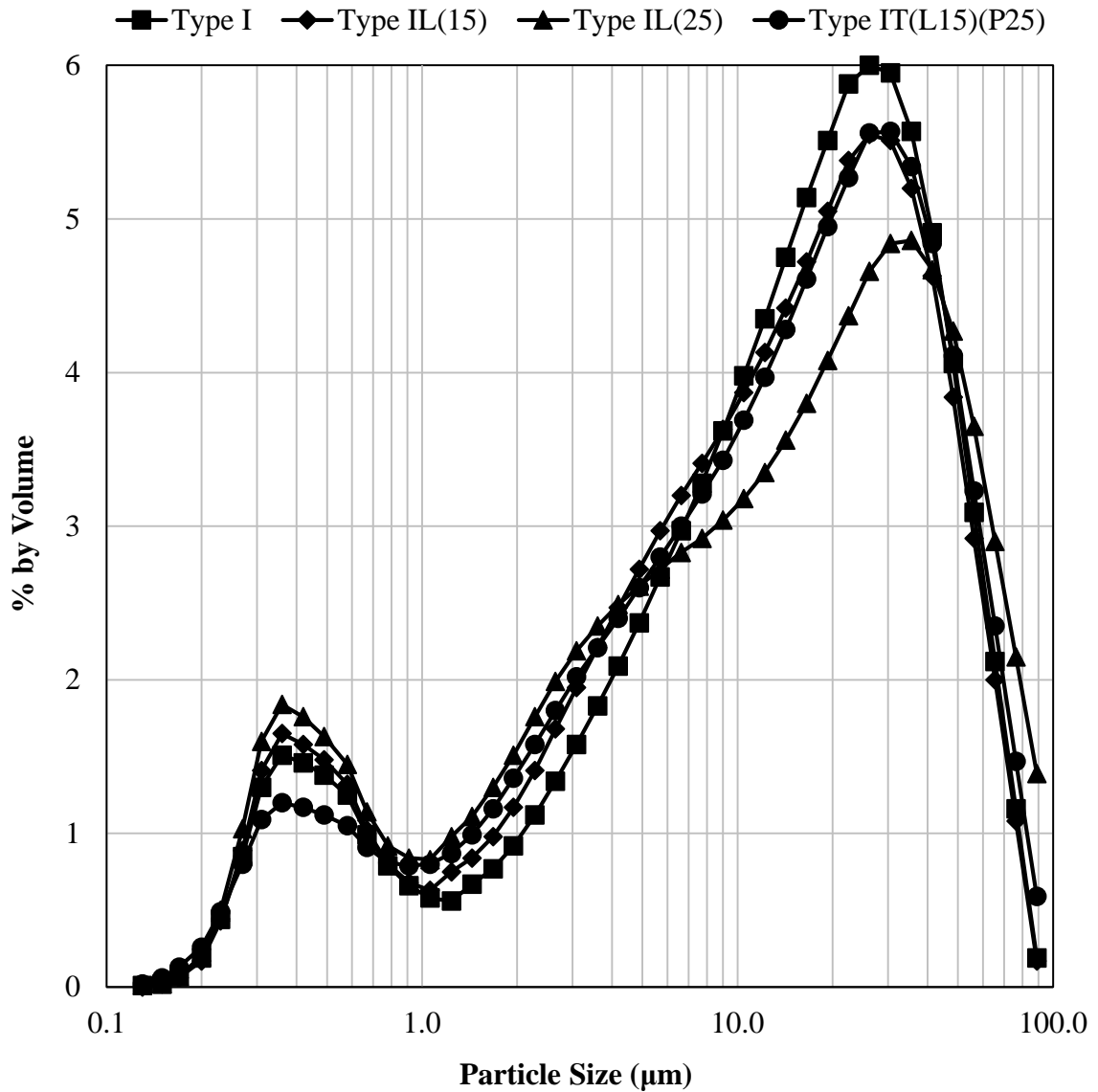


Figure 2.3 Particle Size Distribution of Cement.

2.4 X-Ray Diffraction

2.4.1 Background

X-ray diffraction is used to determine the crystalline structure of materials to identify their chemical composition. This characterization method is based on the phenomenon of wave interference, whereby electromagnetic waves either constructively

or destructively interfere depending on their phase difference. Figure 2.4 shows the diffraction of X-rays by crystal planes. The diffracted beam must satisfy Bragg's Law in order to be in phase (Leng, 2008):

$$n\lambda = 2d \sin \theta$$

where:

- n = order of reflection
- λ = wavelength, nm
- d = spacing between planes, nm
- θ = incident angle, degrees

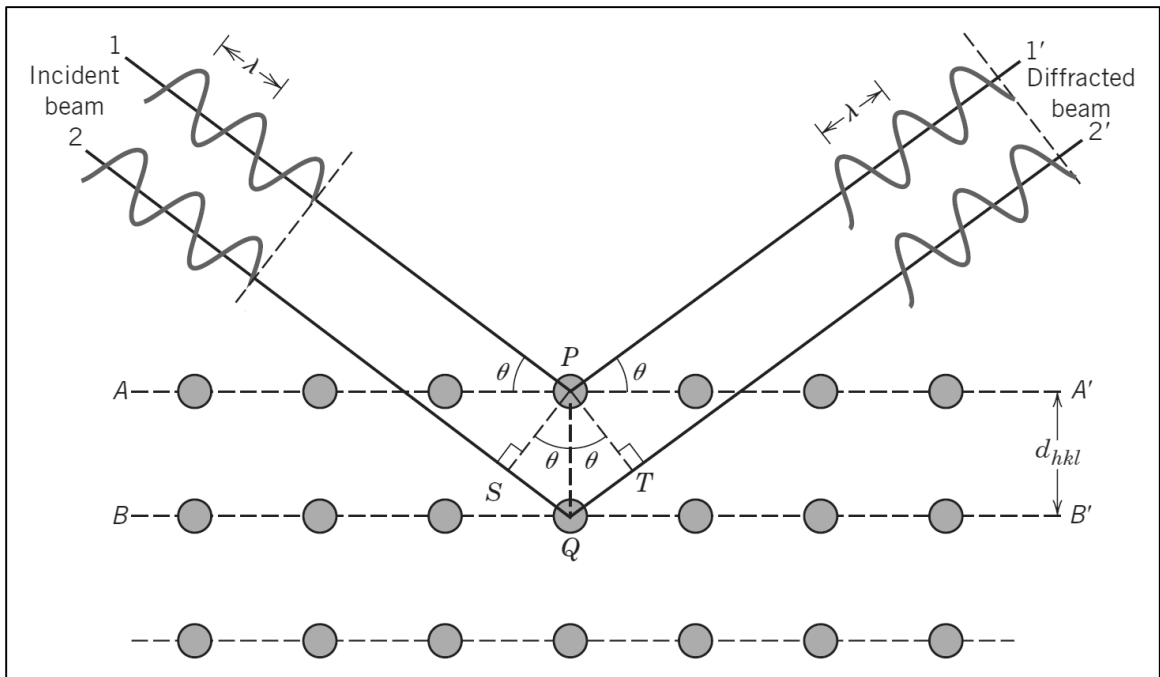


Figure 2.4 Diffraction of X-Rays by Crystal Planes (Callister & Rethwisch, 2010).

The dominant crystalline phase in cement is tricalcium silicate, also known as alite. Many polymorphs of this compound exist as a result of phase transitions that occur during heating and cooling, including triclinic, monoclinic and rhombohedral phases. The crystalline structure of alite is depicted in Figure 2.5, showing calcium and silica

polyhedra in dark and light gray, respectively. The distorted calcium octahedra strips are linked to each other by corners, and the silica tetrahedra link the strips (Smith, 1999).

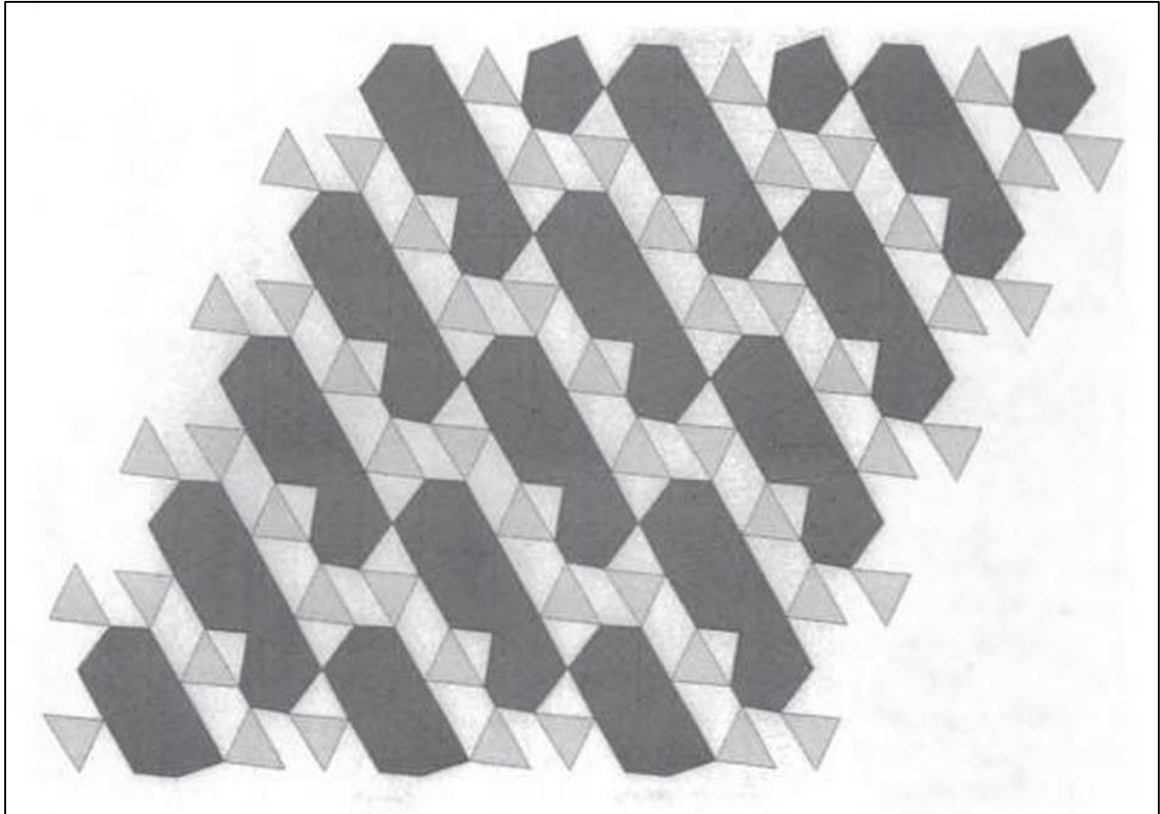


Figure 2.5 Crystalline Structure of Alite (Smith, 1999).

The X-ray diffraction patterns of cement and its primary phases are shown in Figure 2.6. From top to bottom are the measured intensities for cement, alite, tetracalcium aluminoferrite, belite, tricalcium aluminate and calcium oxide. A high degree of overlap occurs between 28° and 36° , making quantitative analysis of cement phases challenging (Smith, 1999).

The inclusion of limestone and fly ash in blended cements makes X-ray diffraction analysis even more complex. However, it is commonly known that the primary crystalline component of limestone is calcium carbonate. The most stable

polymorph of calcium carbonate is calcite, which has a hexagonal crystal structure.

Powder diffraction indicates that the most intense peak for calcite is measured at 29.4° and will create additional overlapping when combined with cement (RRUFF, 2015).

Crystalline silica also has a hexagonal structure and is known to be the main crystalline phase of fly ash. Its main diffraction peak is measured at 26.6° (Kotwal et al., 2014).

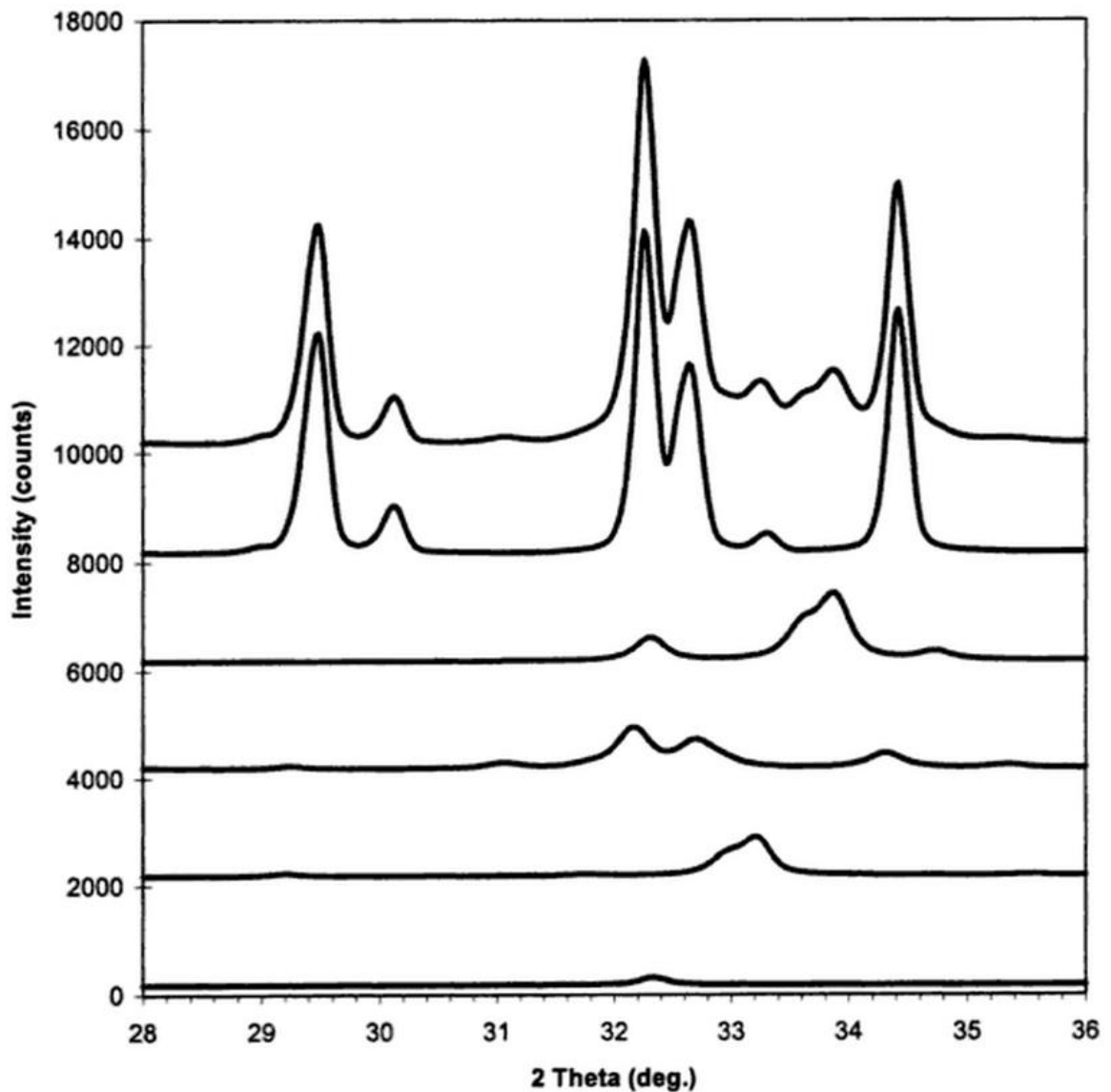


Figure 2.6 X-Ray Diffraction of Cement and Primary Phases (Smith, 1999).

2.4.2 Methodology and Results

The Bruker D8 Advance Eco A25 diffractometer displayed in Figure 2.7 was used for measuring the X-ray diffraction pattern of the cement powders. A thin and level layer of cement was placed on the stage in the center of the apparatus for determination of its crystalline structure. Figure 2.8 illustrates the diffraction patterns of the blended cements. The primary crystalline component was alite, which is characterized by the peaks shown for Type I cement. As the limestone content increased, the sharp peak at 29.4° intensified. This increase in intensity is indicative of calcium carbonate, the main crystalline component of limestone. A small peak at 26.6° was detected in the ternary blend due to the crystalline silica contained in fly ash. X-ray diffraction qualitatively confirmed the chemical composition of the blended cements, but further analysis was needed to quantify the primary cement phases.

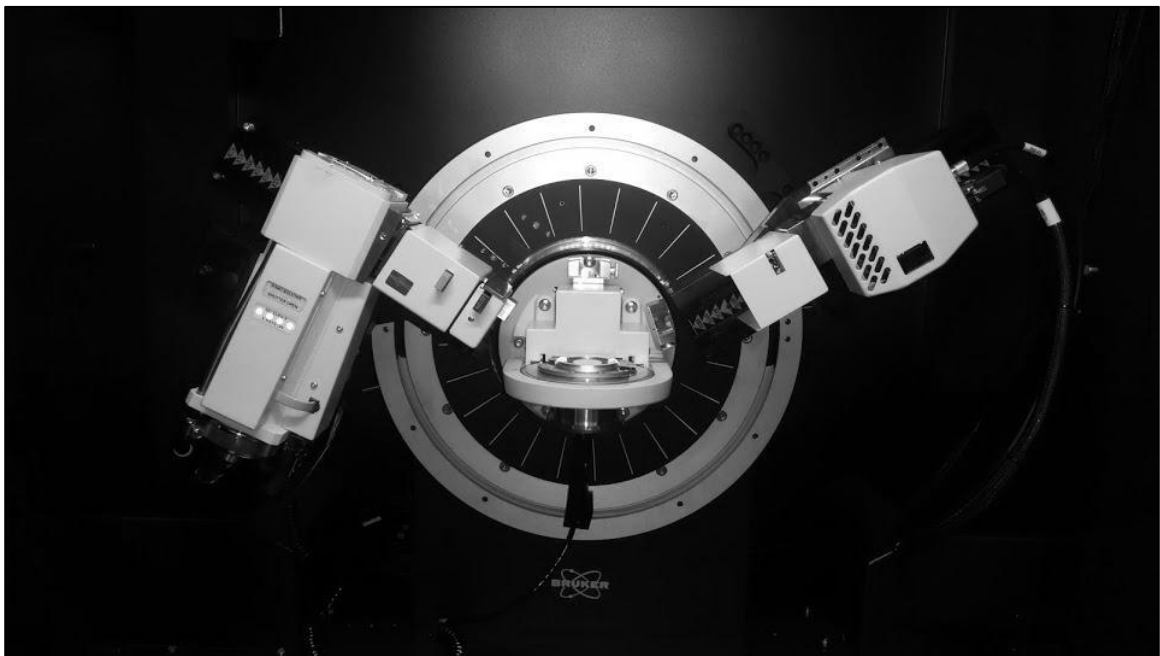


Figure 2.7 Bruker D8 Advanced Eco A25 Diffractometer.

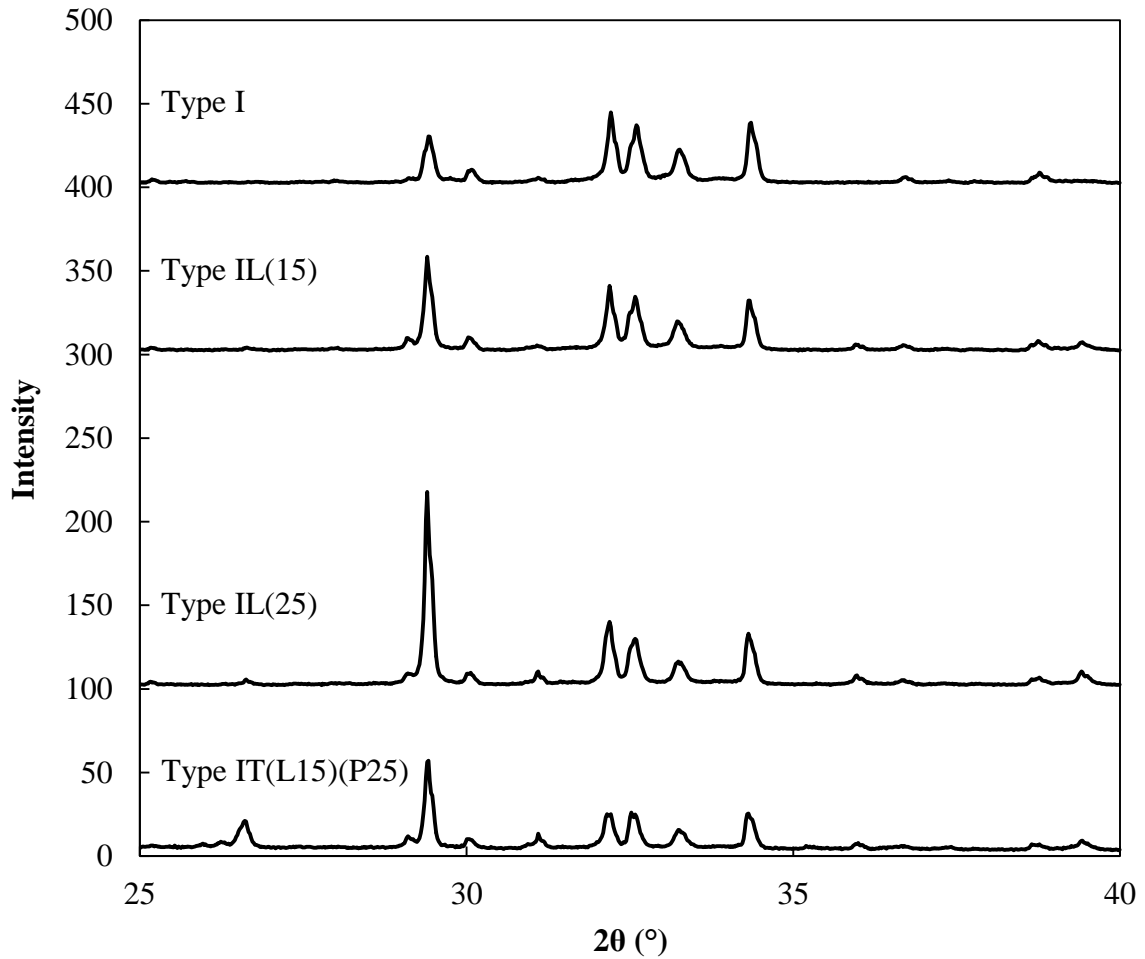


Figure 2.8 X-Ray Diffraction of Cement.

2.5 X-Ray Fluorescence

2.5.1 Background

X-ray fluorescence spectrometry is a characterization method used frequently in the cement industry for quantitative chemical analysis. This technique detects elements by analyzing photon wavelengths or energies that are emitted from a specimen that is radiated with incident X-rays. The wavelength dispersive method is typically employed, as it provides better resolution and a wider elemental analysis range. This is

accomplished by rotating an analyzing crystal and photon counter to align and collect a diffracted beam, which is quantified in accordance with Bragg's Law (Leng, 2008).

Based on the elemental analysis, the composition of the cement is first expressed as oxides by mass percentage. The percentages of alite, belite, tricalcium aluminate and tetracalcium aluminoferrite are then calculated using the Bogue equations provided in ASTM C150 (2012):

$$C_3S = (4.071 \times \%CaO) - (7.600 \times \%SiO_2) - (6.718 \times \%Al_2O_3) - (1.430 \times \%Fe_2O_3) - (2.852 \times \%SO_3)$$

$$C_2S = (2.867 \times \%SiO_2) - (0.7544 \times \%C_3S)$$

$$C_3A = (2.650 \times \%Al_2O_3) - (1.692 \times \%Fe_2O_3)$$

$$C_4AF = (3.043 \times \%Fe_2O_3)$$

where:

- C_3S = alite (tricalcium silicate), mass percentage
- C_2S = belite (dicalcium silicate), mass percentage
- C_3A = tricalcium aluminate, mass percentage
- C_4AF = tetracalcium aluminoferrite, mass percentage

When limestone or inorganic processing additions are combined with the base cement, the content of alite, belite, tricalcium aluminate and tetracalcium aluminoferrite are adjusted as follows:

$$X_f = X_b \times \frac{(100 - L - P)}{100}$$

where:

- X_f = C_3S , C_2S , C_3A or C_4AF in finished cement, mass percentage
- X_b = C_3S , C_2S , C_3A or C_4AF in base cement, mass percentage
- L = limestone, mass percentage
- P = inorganic processing addition, mass percentage

2.5.2 Methodology and Results

Wavelength dispersive X-ray fluorescence of the cement was determined with the Panalytical Axios spectrometer shown in Figure 2.9. Pressed pellet specimens were prepared for the chemical analysis method to provide a level and stable surface. Tables 2.3 and 2.4 present the results of the X-ray fluorescence test after oxides and primary cement phases were formulated from the data collection system. As a result of intergrinding additional limestone, the mass percentage of calcium oxide increased slightly as the corresponding aluminum and silicon oxides decreased. The values differed greatly in the ternary blend due to the high amounts of aluminum and silicon oxides in fly ash, causing the percentage of calcium oxide to decrease. All other oxides detected in the blended cements were within the acceptable range for Type I and do not vary substantially. Based on the small amounts of sodium and potassium oxides, all cement types met the specified optional composition requirements for low-alkali cement.



Figure 2.9 Panalytical Axios X-Ray Fluorescence Spectrometer.

Table 2.3 Oxide Compounds of Cement.

Oxide	Type I (% by Mass)	Type IL(15) (% by Mass)	Type IL(25) (% by Mass)	Type IT(L15)(P25) (% by Mass)
CaO	63.57	65.55	66.41	41.30
SiO ₂	20.07	17.31	15.89	31.13
Al ₂ O ₃	5.40	4.51	3.81	13.92
SO ₃	3.89	3.77	3.75	3.65
Fe ₂ O ₃	1.72	1.60	1.50	2.52
MgO	1.08	1.03	0.91	1.31
K ₂ O	0.66	0.59	0.58	0.65
TiO ₂	0.25	0.23	0.21	0.67
P ₂ O ₅	0.21	0.17	0.17	0.22
Na ₂ O	0.10	0.08	0.08	0.11
SrO	0.10	0.10	0.09	0.10
Mn ₂ O ₃	0.03	0.03	0.03	0.03
ZnO	0.00	0.01	0.01	0.01

The primary phases of the Type I cement were calculated using the Bogue equations. With Type I as the base cement, the phases present in the blended cements were adjusted accordingly. As more limestone and fly ash were interground, the amount of alite, belite, tricalcium aluminate and tetracalcium aluminoferrite decreased. The reduction in mass of the primary phases suggested that the blended cements would be less reactive, potentially causing delayed setting time and lower early age strength.

Table 2.4 Primary Phases of Cement.

Phase	Type I (% by Mass)	Type IL(15) (% by Mass)	Type IL(25) (% by Mass)	Type IT(L15)(P25) (% by Mass)
C ₃ S	56.43	48.87	43.23	35.44
C ₂ S	14.97	12.96	11.47	9.40
C ₃ A	11.40	9.87	8.73	7.16
C ₄ AF	5.23	4.53	4.01	3.29

2.6 Specific Gravity

2.6.1 Background

The specific gravity of all the constituent materials used in mortar and concrete are essential when calculating volumetric mixture proportions. This is particularly important for blended cements, as the specific gravity changes when high volumes of limestone and fly ash are incorporated. This variation must be accounted for in order to maintain a consistent volume of material and prevent underyielding or overyielding.

2.6.2 Methodology and Results

The specific gravity of each cement type was calculated using the relative density and mass percentage of the constituents. The results are shown in Table 2.5 based on the interground limestone and Class F fly ash having relative densities of 2.71 and 2.32, respectively. The specific gravity decreased from 3.15 to 2.89 as a consequence of incorporating larger quantities of the mineral admixtures. The lower specific gravity of the blended cements indicated that the materials were less dense and would occupy a larger volume for a given mass. Therefore, an overyield of material was likely to occur if the variation was not taken into consideration for volumetric mix design calculations.

Table 2.5 Specific Gravity of Cement.

Cement Type	Specific Gravity
I	3.15
IL(15)	3.09
IL(25)	3.05
IT(L15)(P25)	2.89

III. AGGREGATE

3.1 Overview

Although the primary focus of this study was on blended cements, the importance of aggregates in concrete should not be understated. Aggregates are considered to be economical fillers and occupy the largest portion of the concrete matrix. As a result, concrete properties are greatly impacted by aggregate gradation and composition. Aggregates influence the water demand and workability of fresh concrete as well as the density, strength and durability of hardened concrete. Therefore, the characteristics of the aggregates must be determined.

For this study, Ottawa sand consisting of nearly pure quartz was used as the fine aggregate in all mortar mixtures. River sand and crushed limestone were used as the fine and coarse aggregates in all concrete mixtures. The river sand was siliceous, whereas the crushed limestone was calcareous with respect to its composition. The characteristics of the aggregates were determined to ensure quality control of the mixtures and to verify that each material conformed to its respective specification.

3.2 Sieve Analysis

3.2.1 Background

The particle size distribution of aggregate is a critical factor that affects the performance of fresh and hardened concrete (ACI E701, 2007). Figure 3.1 illustrates the difference between well graded, poorly graded and gap graded aggregate. Well graded aggregate is preferred as it provides improved particle packing and maximizes the efficiency of the cement.

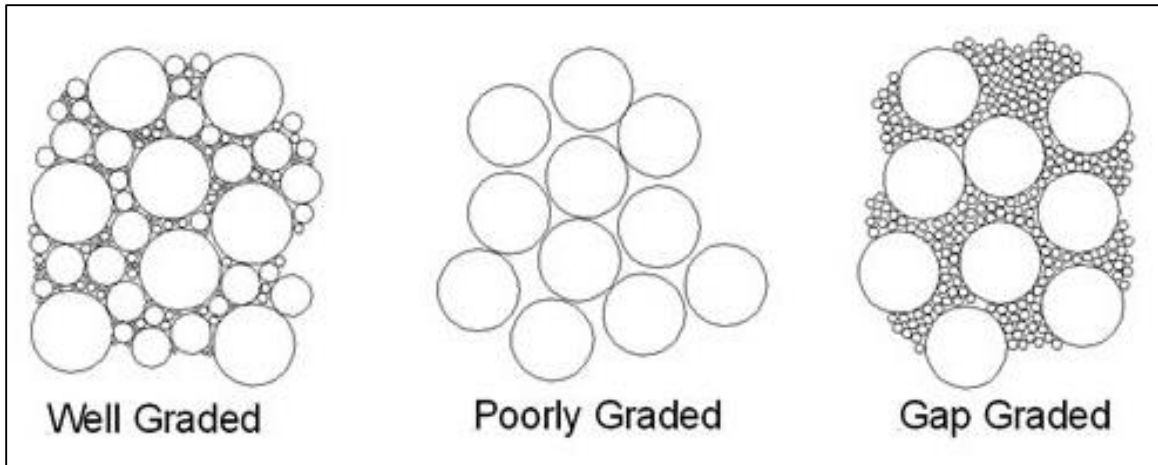


Figure 3.1 Aggregate Gradations (Civil Engineers Forum, 2015).

Care must be taken when sampling aggregates for testing to ensure that representative samples are obtained. Sampling aggregate is performed according to the standard practice in ASTM D75 (2014), where samples are taken from the top third, midpoint and bottom third of the stockpile elevation. Using a representative sample of appropriate mass based on the nominal maximum aggregate size, sieves with suitable size openings are used to determine gradation.

3.2.2 Methodology and Results

A sieve analysis of the aggregate was performed in accordance with ASTM C136 (2006) by passing the material through appropriately sized sifters. Figure 3.2 shows the results of the sieve analysis. The gradation of the Ottawa sand conformed to the requirements for graded standard silica sand as per ASTM C778 (2013). Test results also indicated that the river sand met the specifications for fine aggregate, and the crushed limestone was classified as a #57 coarse aggregate as outlined in ASTM C33 (2013).

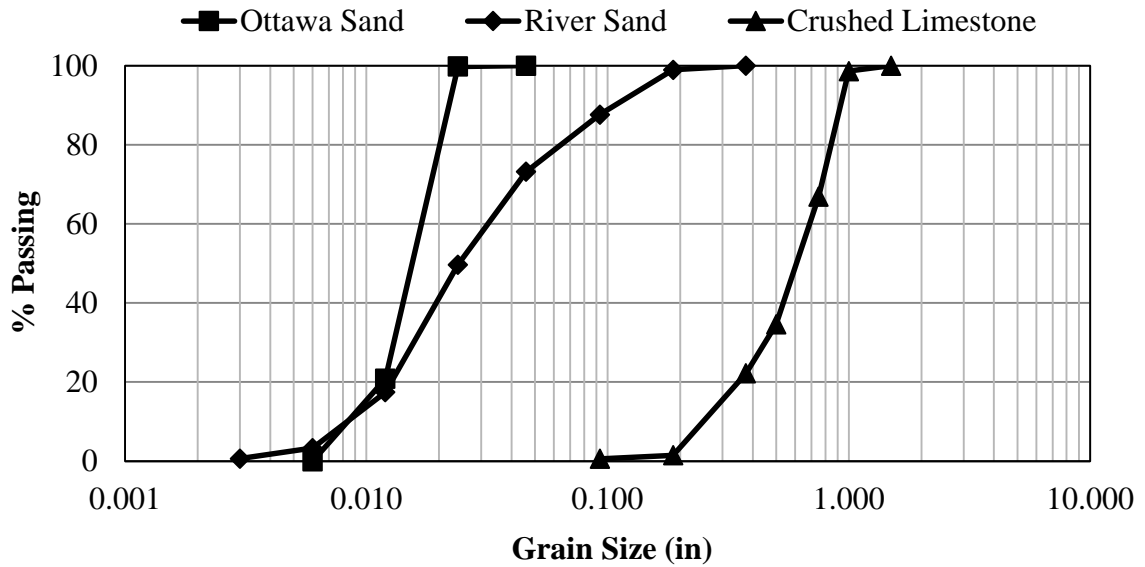


Figure 3.2 Sieve Analysis of Aggregate.

3.3 Specific Gravity and Absorption

3.3.1 Background

Normal-weight aggregate has a specific gravity between 2.4 and 2.9. Variations in the relative density occur as a result of chemical composition and voids that may or may not contain water (Kosmatka et al., 2003). As per Figure 3.3, aggregate can exist in four different moisture conditions: oven dry (OD), air dry (AD), saturated surface dry (SSD) and wet (W).

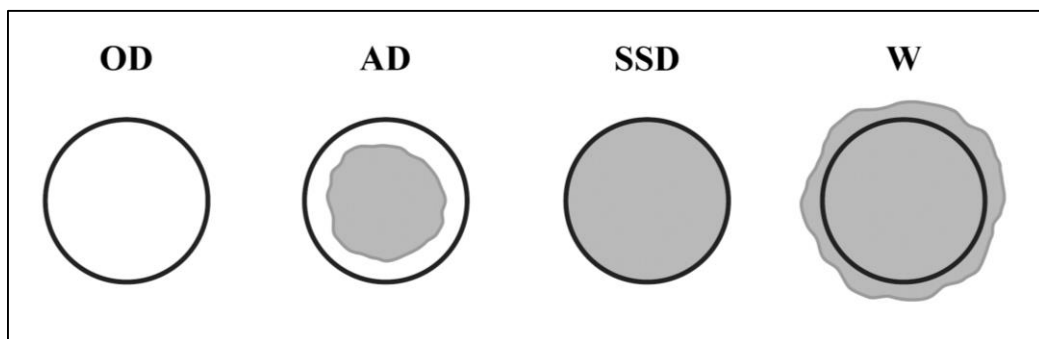


Figure 3.3 Moisture Conditions of Aggregate.

In oven dry and saturated surface dry conditions, the specific gravity is calculated as follows (ASTM C127, 2012):

$$OD \text{ Specific Gravity} = \frac{A}{B - C}$$

$$SSD \text{ Specific Gravity} = \frac{B}{B - C}$$

where:

- A = mass of oven dry sample, g
- B = mass of saturated surface dry sample, g
- C = mass of saturated sample in water, g

In air dry or wet conditions, aggregate is capable of absorbing water from or contributing water to a concrete mixture. Common absorption levels are in the range of 0.2% to 4.0% (Kosmatka et al., 2003). To confirm that the total water allocated for each mixture remains constant, it is necessary to measure the aggregate absorption using the aforementioned fixed conditions as well as the moisture content in its original state. By using the following absorption and moisture content calculations, the amount of mixing water is proportioned accordingly (ASTM C127, 2012; ASTM C566, 2013):

$$Absorption (\%) = \frac{B - A}{A} \times 100$$

$$Moisture Content (\%) = \frac{W - A}{A} \times 100$$

where:

- A = mass of oven dry sample, g
- B = mass of saturated surface dry sample, g
- W = mass of original sample, g

3.3.2 Methodology and Results

The specific gravity and absorption of the fine and coarse aggregates were measured in accordance with ASTM C127 (2012) and ASTM C128 (2012). The test results are presented in Table 3.1. In a saturated surface dry condition, the relative densities ranged from 2.54 to 2.65. Congruent with the respective oven dry and saturated surface dry measurements, the absorption of the aggregates varied from 0.2% to 2.4%. These values were within the typical ranges for normal-weight aggregate and were accounted for when proportioning the mortar and concrete mixtures.

Table 3.1 Specific Gravity and Absorption of Aggregate.

Aggregate	Oven Dry Specific Gravity	Saturated Surface Dry Specific Gravity	Absorption (%)
Ottawa Sand	2.65	2.65	0.2
River Sand	2.56	2.60	1.5
Crushed Limestone	2.48	2.54	2.4

IV. MORTAR

4.1 Overview

The physical properties of mortar are important due to the relation they have with the performance of concrete. For this reason, several tests were conducted without coarse aggregate by only using mixtures of cement, water and Ottawa sand. The purpose was to obtain information regarding the effect of the blended cements on the properties of fresh and hardened mortar and to compare the results to Type I cement and relevant specifications.

Constituent materials were proportioned in accordance with applicable standard test methods. If standard mixture proportions were not specified, recommended practices of the cement manufacturer were followed. Material and environmental factors were controlled to ensure that the only variable in the mixtures was the cement type. Depending on the required batch volume, the mortar was mixed with either a 5 qt or 20 qt planetary mixer by following the ASTM C305 (2014) practice for mechanical mixing of hydraulic cement mortar of plastic consistency.

4.2 Flow

4.2.1 Background

The flow of fresh mortar is considered to be related to the workability and finishability of concrete. It is calculated by measuring the increase in diameter of mortar that is released from a flow mold and spread out on a flow table. A sufficient flow results in a spread that is approximately $110\% \pm 5\%$ larger than the original base diameter.

Conflicting results for mortar flow have been described in the scientific literature regarding portland limestone cement. The variation is based on the influence of particle size on water demand. A narrow particle size distribution demands a higher water content to produce comparable results. However, a wide particle size distribution leads to reduced water demand, since gaps are filled between larger cement particles (Detwiler, 1995).

Although particle size has been cited as the primary factor, Sprung & Siebel (1991) determined that the amount of clay in the limestone also affects flow. If the methylene blue index for clay content is too high, the water demand exceeds the values that would be expected from a narrow particle size distribution alone. As a consequence, the ASTM C595 (2013) requirements for limestone in blended cement dictate that the methylene blue index be limited to 1.2 g per 100 g.

4.2.2 Methodology and Results

The flow of mortar was measured using a flow table as per ASTM C1437 (2013). The spread was expressed as the percentage increase of the original base diameter of the mortar released from a flow mold. Table 4.1 indicates that the test results ranged from 104% to 109%. These measurements signified no considerable variation in flow and suggested that concrete based on the blended cements would perform in a similar manner.

Table 4.1 Flow of Mortar.

Cement Type	Flow (%)
I	104
IL(15)	109
IL(25)	106
IT(L15)(P25)	109

4.3 Isothermal Calorimetry

4.3.1 Background

Measuring the heat of hydration is an effective method for evaluating the exothermic reaction that occurs during the reaction of cement with water. Isothermal calorimetry is used in the cement industry to measure heat generation and to predict setting time and early age strength development. It also provides an indication of the stability of the material after heating and subsequent cooling. When heat is not rapidly dissipated, undesirable tensile stresses develop from non-uniform cooling. The heat generation rate is largely influenced by the chemical composition of the cement. Alite and tricalcium aluminate are primarily responsible for heat evolution, although consideration must also be given to the fineness of the particles, curing temperature, water-cement ratio and calcium sulfate content. The largest amount of thermal energy is generated within the first day, but the hydration process may continue for many years (Copeland et al., 1960).

Previous research has shown that heat generation increases when limestone is used in addition to cement. However, if limestone is used as a partial replacement for cement, then heat decreases. Hooton (1990) investigated the effect of limestone on the heat of hydration. When replacing 5% of the cement with limestone, the researcher found little to no effect on the heat of hydration.

Livesey (1991) also studied the performance of portland limestone cement using isothermal calorimetry. The results of the study indicated that the rate and total amount of heat reduced by increasing limestone content. Conversely, the exothermic reaction accelerated when the cement had a higher surface area.

4.3.2 Methodology and Results

The Calmetrix I-Cal 8000 isothermal calorimeter with CalCommander software presented in Figure 4.1 recorded the heat flow generated by the early hydration reaction of cement in mortar as the ambient temperature around the samples was controlled. As per Figure 4.2, the more prominent initial rate of thermal energy generated by Type I cement after a hydration time of 0.5 hours resulted from a higher content of tricalcium aluminate. This heat flow peak exhibited decreased power as the amount of limestone increased. A predictable trend was also observed during the hydration of the alite phase after a hydration time of about 7 hours. More limestone and fly ash resulted in less energy being produced, suggesting that the mortar would have delayed setting time and decreased early age strength.

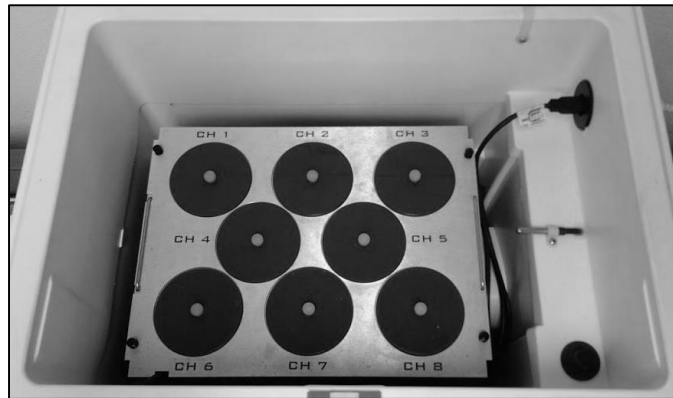


Figure 4.1 Calmetrix I-Cal 8000 Isothermal Calorimeter.

A variation was also found to be related to the hydration reaction of calcium sulfate with tricalcium aluminate. The aluminate phase reacted quickly and then became stable as the sulfate formed a barrier of ettringite around the particles. This barrier allowed the reaction to proceed at a controlled rate. Eventually, the barrier was broken down when the aluminate phase depleted the sulfate, converting the ettringite to

monosulfoaluminate and allowing the tricalcium aluminate to react rapidly again. For mortar based on Type I, the sulfate depletion peak appeared as a shoulder or brief plateau immediately following the main peak. With larger amounts of limestone, a substantial impact was found to be the increased duration between the main hydration peak and the later sulfate depletion peak. A longer interval between the peaks typically corresponds with increased setting time and lower early age strength.

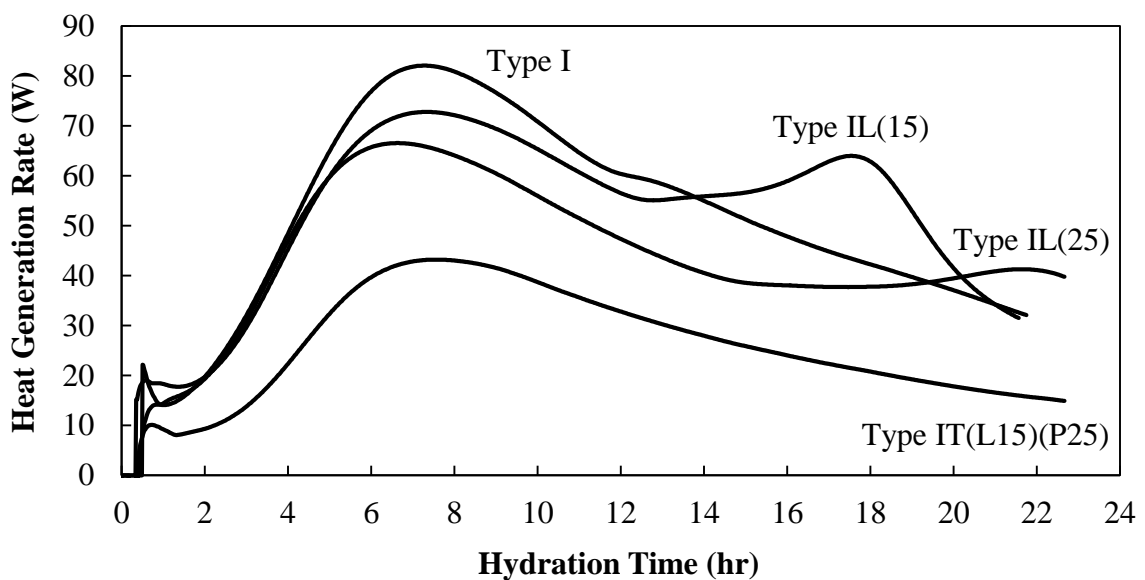


Figure 4.2 Heat Generation of Mortar.

4.4 Setting Time

4.4.1 Background

During construction, setting time affects the transport and placement of fresh concrete. The point at which formwork can be removed and the concrete bears a load are also a function of setting time. Setting time is slowed and hardened properties are improved by supplementing cement clinker with calcium sulfate in the final milling stage of the cement manufacturing process (Tang, 1992).

The objective of a setting time test is to determine the moment from when the cement is hydrated until the paste ceases to be plastic and achieves a certain degree of hardness. Initial and final setting times are measured with a Vicat apparatus, Gillmore needle or Acme mortar penetrometer. With a penetrometer, the initial and final setting times are defined as the elapsed time required for mortar to achieve a penetration resistance of 500 psi and 4000 psi, respectively (ASTM C403, 2008). According to ASTM C150 (2012), the initial setting time should not be less than 45 minutes or more than 375 minutes.

Prior studies on the use of limestone in cement at levels up to 15% have presented inconsistent results for setting time. Some researchers have reported an increase in setting time, whereas others have found that limestone decreases the time required for hardening to occur. The variation in outcomes is attributed to the manufacturing method and the use of portland limestone cement with differing chemical composition and particle size (Tennis et al., 2011).

4.4.2 Methodology and Results

Penetration resistance was used to determine the initial and final setting times of mortar as defined in ASTM C403 (2008). The Acme mortar penetrometer displayed in Figure 4.3 was used for this test. Figure 4.4 indicates the average results of three specimens for each cement type. The initial setting time range was between 3.5 hours and 6 hours, and the corresponding final setting time ranged from 5 hours to 9 hours. Compared to Type I cement, the setting time of the blended cements increased with larger quantities of limestone. Only a slight increase in setting time was measured for Type IL(25) when compared to Type IL(15), but the variation was found to be

statistically significant ($p < 0.05$). The fly ash substantially hindered the setting time of Type IT(L15)(P25) due to its delayed reactivity with calcium hydroxide. The results of the penetration resistance test were within the anticipated range and provided a good indication of what trend to expect for the early age strength development of mortar.



Figure 4.3 Acme Mortar Penetrometer.

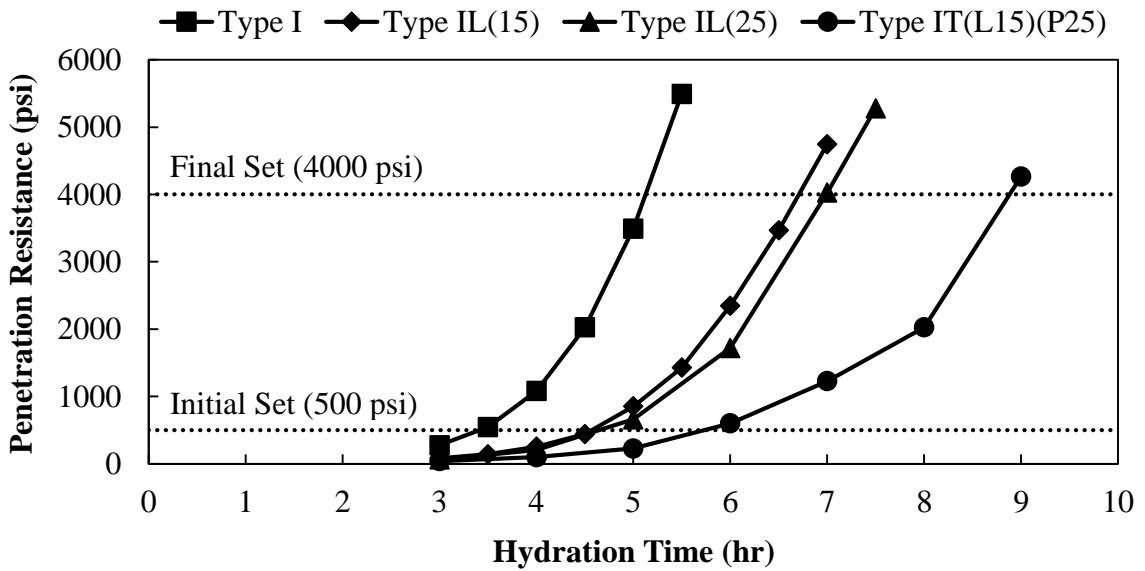


Figure 4.4 Setting Time of Mortar.

4.5 Compressive Strength

4.5.1 Background

The compressive strength of mortar is one of the most common test methods used to measure mechanical behavior after the mortar has hardened. It is determined by applying a uniaxial load to mortar cubes until failure at various ages. Compressive strength is computed by dividing the maximum applied load by the cross sectional area of the test specimen. The result of the calculation must comply with the minimum requirements designated by the corresponding ASTM specifications shown in Table 4.2.

Table 4.2 Specified Compressive Strength of Mortar.

Cement Type	ASTM	3 Day Strength (psi)	7 Day Strength (psi)	28 Day Strength (psi)
I	C150	1,740	2,760	4,060
IL(15)	C595	1,890	2,900	3,620
IL(25)	C1157	1,890	2,900	4,060
IT(L15)(P25)	C1157	1,890	2,900	4,060

When hardened mortar is cured in a humid environment, strength gain continues to occur provided that unhydrated cement is present in the mixture. If mortar is reintroduced to a saturated environment after a drying period, hydration of cement resumes and strength will continue to increase. Other factors also affect hydration, such as temperature, admixtures and sufficient space for water within the cement matrix (Powers, 1948).

Sprung & Siebel (1991) found that compressive strength is not typically reduced when using 5% to 10% limestone in blended cements. If larger quantities of limestone are used, the strength may decrease compared to ordinary cement as a function of Blaine

fineness, particle size distribution and chemical composition. Loss of strength resulting from the dilution of the base cement can be mitigated by finer grinding in the final milling stage (Schmidt, 1992).

4.5.2 Methodology and Results

The compressive strength of 2 in. mortar cubes was measured in accordance with ASTM C109 (2013) at ages of 1, 3, 7, 28 and 90 days using the test setup shown in Figure 4.5.



Figure 4.5 Setup for Compressing Mortar.

Figure 4.6 depicts the average compressive strength of three test specimens at each test age. Mortar with Type IL(15) reached strengths at 1 and 3 days that were comparable to Type I. Slightly lower strengths were measured at 7, 28 and 90 days. Mortar based on Type IL(25) exhibited further decreases in strength throughout the 90 day test period due to its higher limestone content. Although similar 28 day strength was measured for Type IL(25) and Type IT(L15)(P25) based mortars, the ternary blend had substantially lower early age strength and higher late age strength. The slower strength gain rate resulted from the delayed formation of fly ash hydration products.

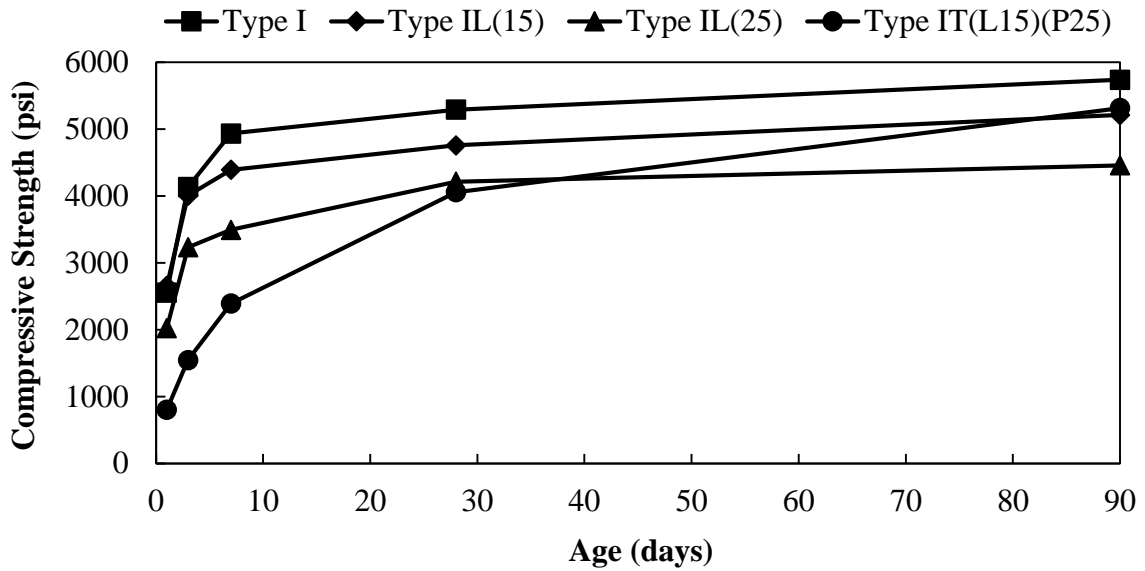


Figure 4.6 Compressive Strength of Mortar.

As discussed in the background section, ASTM provides minimum compressive strength requirements for mortar at ages of 3, 7 and 28 days. Table 4.3 was used to compare the test results to the strength requirements to verify compliance. Type GU for general construction as described in ASTM 1157 (2011) was the basis for evaluating Type IL(25) and Type IT(L15)(P25). With the exception of Type IT(L15)(P25), all cement types exceeded the specified strengths at each age. Although the ternary blend did not meet specification at 3 and 7 days, its strength increased by 28 days to fulfill the physical requirement.

Table 4.3 Compressive Strength of Mortar.

Cement Type	3 Day Strength (psi)	7 Day Strength (psi)	28 Day Strength (psi)
I	4,130	4,930	5,290
IL(15)	4,010	4,390	4,760
IL(25)	3,230	3,490	4,210
IT(L15)(P25)	1,550	2,390	4,060

4.6 Drying Shrinkage

4.6.1 Background

Hardened mortar changes volume due to influential factors such as temperature, humidity or stress (CCAA, 2002). Mortar that is continually kept moist will slightly expand. When it is permitted to dry, mortar will shrink and potentially crack from the stress if it is restrained (Kosmatka et al., 2003). Previous studies on the drying shrinkage of portland limestone cement have found little to no change in volume due to the addition of small amounts of limestone (Detwiler, 1996). The purpose of this test was to evaluate the effect of blended cements with high volume interground limestone on the drying shrinkage of mortar.

4.6.2 Methodology and Results

The drying shrinkage of 1×1×10 in. mortar prisms was determined as per ASTM C596 (2009) using a length comparator with digital indicator. Figure 4.7 displays an image of the test specimens and apparatus.



Figure 4.7 Length Comparator and Mortar Prisms.

The average results of drying shrinkage over 90 days for four test specimens are shown in Figure 4.8. Mortar prisms for all cement types shrank approximately the same amount during the first 25 days of air storage with an average length change of 0.09%. However, the divergence in the 90 day measurements, ranging from 0.11% to 0.14%, suggested that long term drying shrinkage decreased slightly for cement containing higher volumes of limestone and fly ash. An analysis of variance confirmed that the main effect of cement type on drying shrinkage was statistically significant ($p < 0.05$) at 90 days. A reduction in length change typically corresponds with improved volumetric stability and lower potential for cracking.

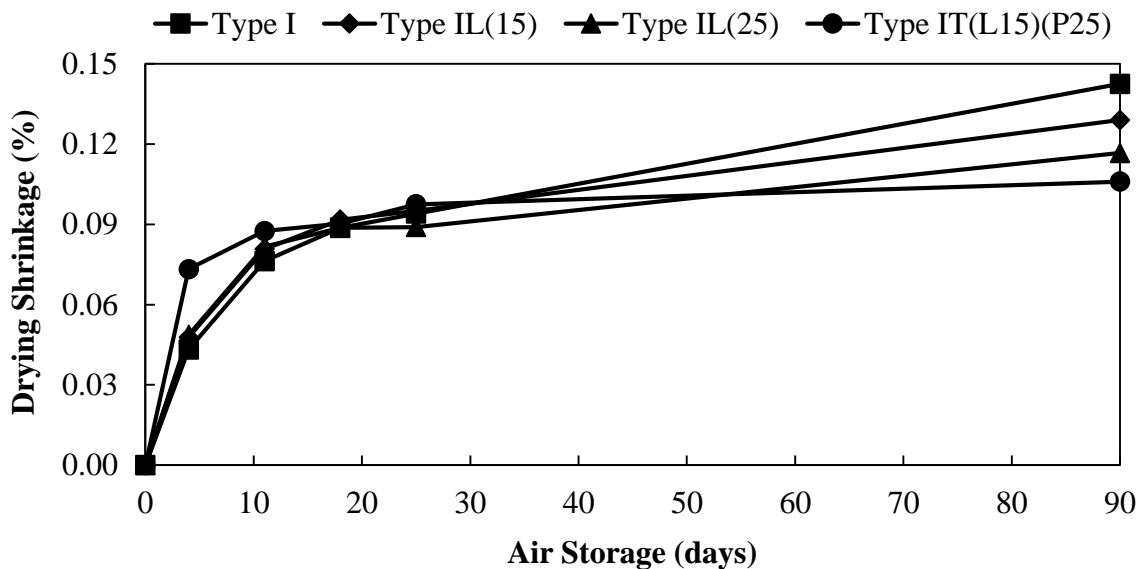


Figure 4.8 Drying Shrinkage of Mortar.

4.7 Sulfate Expansion

4.7.1 Background

Chemicals in the surrounding environment also cause volumetric changes when they adversely react with cement. Soils and groundwater with excessive amounts of

sulfate ions react with the calcium hydroxide and aluminate phases, forming calcium sulfate, ettringite and other expansive compounds that create internal pressure (Neville, 2006). The internal pressure results in disintegration of the cement matrix by inhibiting cohesion. In the presence of sodium sulfate, calcium sulfate or magnesium sulfate, the binder decomposes and loses strength (Santhanam et al., 2001).

A particular concern for portland limestone cement is the formation of the thaumasite form of sulfate attack. Thaumasite is an expansive compound that has increased potential to damage cement with limestone, especially in cold and wet environments (Hawkins et al., 2003). In a study on sulfate attack in the United Kingdom, Crammond (2003) stated that the susceptibility of cement to expand from thaumasite increases in relation to the amount of interground limestone.

Drimalas et al. (2011) evaluated sulfate attack for the Texas Department of Transportation through laboratory and field testing. The researchers found that Texas soils predominately contain calcium sulfate, which is less aggressive than sodium sulfate due to its lower solubility. Although this finding limits the external validity of using sodium sulfate for laboratory testing in Texas, ASTM procedures are still recommended for determining the resistance of cement to sulfate attack.

4.7.2 Methodology and Results

A length comparator with digital indicator was used to measure the expansion of 1×1×10 in. mortar prisms exposed to sodium sulfate solution in accordance with ASTM C1012 (2013). Two rounds of testing were performed with six specimens for each cement type. Specimens were monitored for an exposure period of 6 months. The tests were found to be inconclusive based on the variation in the results.

V. CONCRETE

5.1 Overview

The engineering properties of concrete were evaluated to substantiate the use of blended cements for construction applications. Several tests were performed using mixtures of cement, water, river sand and #57 crushed limestone. The purpose was to obtain information regarding the effect of the blended cements on the properties of fresh and hardened concrete and to compare the results to Type I cement and relevant specifications.

Concrete mixtures were proportioned in accordance with recommendations provided by the cement manufacturer. Material and environmental factors were controlled to ensure that the only variable in the mixtures was the cement type. Each batch of concrete was mixed with the 6 ft³ Crown C6 concrete drum mixer shown in Figure 5.1 by following the ASTM C192 (2014) practice for making concrete in the laboratory.



Figure 5.1 Crown C6 Concrete Drum Mixer.

Table 5.1 indicates the volume percentage of the constituent materials and target air content for all batches produced. The actual batch weights for each constituent varied based on the specified gravity of the blended cement and the moisture content of the aggregates. To maintain a consistent paste volume and water-cement ratio, the proportions of cement and water were adjusted accordingly.

Table 5.1 Volumetric Concrete Mix Design.

Material	Volume (%)
Cement	9.8 - 10.3
Water	16.4 - 16.9
River Sand	27.1
Crushed Limestone	40.7
Target Air Content	5.5

5.2 Fresh Concrete Properties

5.2.1 Background

The slump of fresh concrete provides an indication of its mobility and consistency. It is measured as the subsidence of fresh concrete from a slump cone and ranges from about 1 in. to 6 in. depending on the application. Several characteristics of a concrete mixture will affect the measured slump (ACI CP1, 2015). Schmidt et al. (1993) found that fine particles of limestone displaced water in the interstitial sites between the cement and aggregate particles. The displacement of water from the voids provided additional internal lubricant and created concrete mixtures that were less stiff. Thus, less water was needed to make a concrete mixture with desired fluidity. Brookbanks (1993) discovered similar results in his report for the Building Research Establishment when replacing low volumes of cement with limestone.

Ensuring the quality, setting time and strength of concrete is challenging if temperature is not controlled. Performance can be lessened when the initial temperature is outside of an acceptable range, which is 68°F to 86°F for laboratory tests (ASTM C192, 2014). Higher early age strength typically develops in concrete with a high initial temperature, but long term strength may be reduced. A lower initial temperature results in improved long term quality while sacrificing early age strength development (ACI CP1, 2015). Previous studies on portland limestone cement have indicated that lower temperature may lead to the formation of thaumasite, a potential mechanism for deterioration (Hooton & Thomas, 2002).

Normal-weight concrete has a density of approximately 137 lb/ft³ to 150 lb/ft³ (Kosmatka et al., 2003). In a study on innovations in cement manufacturing, Schmidt et al. (2004) concluded that packing density was optimized with the use of 15% limestone. Since cement ultimately accounts for only a small portion of a concrete mixture, the density of fresh concrete is not substantially affected. Nevertheless, density is an important measurement used for quality control to determine the yield of a mixture. The yield is calculated by dividing the mass of the batch materials by the density of the concrete. Based on the actual volume, the relative yield is then calculated as a ratio to the design volume. Undesired consequences result when the relative yield is not equal to 1.00, including financial and performance losses (ASTM C138, 2014).

Conventional concrete has an air content on the order of 1% to 3% due to a small amount of air becoming entrapped during the mixing process. Air-entrained concrete typically has an air content of 4% to 8%. To prevent substantial deterioration from hydraulic pressure during freeze-thaw cycles, air-entraining admixtures create additional

microscopic air voids that allow water to expand and contract (Whiting & Nagi, 1998). In a report by the Federal Highway Administration, Tanesi et al. (2013) indicated that there was no substantial variation in the air content of fresh concrete when using portland limestone cement. Similarly, Brookbanks (1993) found only slight deviations in air content when studying the interaction of limestone with an air-entraining admixture. Yet, when fly ash is included, Hill & Folliard (2006) propose that residual unburned carbon negatively interacts with air-entrainers and requires increased dosage to achieve a target air content.

5.2.2 Methodology and Results

Three concrete batches with a design volume of 2.0 ft³ were mixed for each cement type. Figure 5.2 shows the tools used to measure the properties of each concrete batch.



Figure 5.2 Slump Cone, Thermometer, Air Meter and Associated Tools.

Average values of the fresh concrete properties are presented in Table 5.2. Slump was measured as the subsidence of fresh concrete from a slump cone as described in

ASTM C143 (2012). The average slump of the concrete ranged from 4.75 in. to 5.75 in. These values signified that there was no considerable difference in slump amongst the mixtures and that all average values were within the target range of 4 in. to 6 in.

Table 5.2 Fresh Concrete Properties.

Cement Type	Slump (in)	Temperature (°F)	Density (lb/ft³)	Relative Yield	Air Content (%)
I	4.75	71	139.7	1.00	6.1
IL(15)	5.75	71	140.0	1.00	5.4
IL(25)	5.50	70	140.6	1.00	5.2
IT(L15)(P25)	5.75	71	139.1	1.00	5.1

The fresh concrete temperature was measured as outlined in ASTM C1064 (2012). The test was performed with a stem type thermometer capable of accurately measuring temperature to $\pm 1^\circ\text{F}$ throughout a range of 30°F to 120°F . A temperature of 70°F to 71°F was measured for all concrete mixtures. These results conformed to the requirements of ASTM C192 (2014), which stipulate that the concrete materials must be in the range of 68°F to 86°F .

Using the 0.25 ft^3 measuring bowl from a Type B air meter, the density of the fresh concrete was calculated in accordance with ASTM C138 (2014) by dividing the mass of the concrete by the volume of the measure. The average density varied slightly from 139.1 lb/ft^3 to 140.6 lb/ft^3 but was in the typical range for conventional concrete. Based on the mass of the batch materials and the measured densities, the actual yields were calculated to be 2.0 ft^3 , corresponding to relative yields of 1.00. Thus, the actual volume of the concrete was equal to the design volume.

Air content was measured with a Type B meter having a vertical air chamber as per ASTM C231 (2014). The average air content ranged from 5.1% to 6.1% and was

acceptable for casting test specimens. BASF MasterAir AE 90 air-entraining admixture was used to achieve the target air content. The standard dosage was 0.13 mL/lb of cement. A higher dosage of 1.27 mL/lb of cement was needed in the ternary blend due to the high amount of residual carbon in the fly ash.

5.3 Petrography

5.3.1 Background

Petrographic examination uses microscopes to analyze the quality of hardened concrete and the integrity of the interfacial transition zone between cement paste and aggregate. The concrete matrix is often evaluated to estimate future performance (Kosmatka et al., 2003).

Scanning electron microscopes examine the surface microstructure of materials with high resolution and large depth of field. The instrumentation consists of an electron gun and lenses that focus an electron beam to scan the specimen surface as shown in Figure 5.3. An image is formed by collecting and amplifying emitted electrons from the specimen then reconstructing the signal on a control console (Leng, 2008).

There are two electron signal types used to form images by scanning electron microscopes. The high energy incident electrons result in elastic or inelastic scattering when scanning the specimen surface. Backscattered electrons are produced by elastic scattering of electrons by atoms in a specimen and are useful for elemental analysis. Secondary electrons are produced by inelastic scattering of electrons that are ejected from atoms and are collected to form enhanced topographic contrast (Leng, 2008).

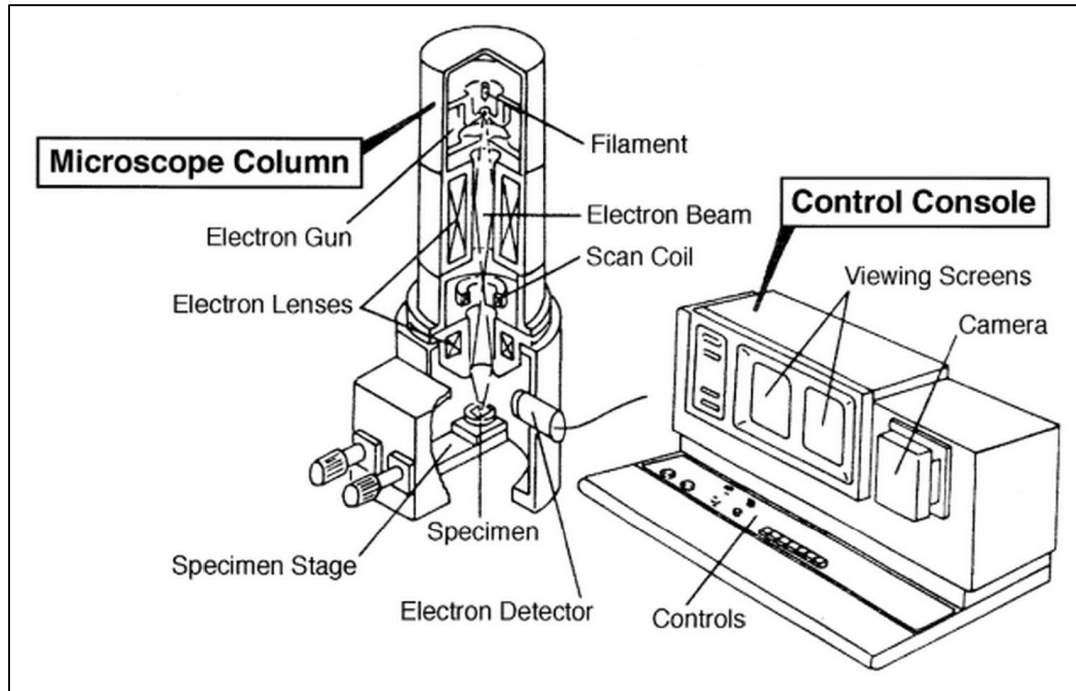


Figure 5.3 Scanning Electron Microscope Column and Control Console (Goldstein et al., 2012).

5.3.2 Methodology and Results

Thin sections were saw cut from 4×8 in. concrete cylinders and manually polished using 2500 grit silicon carbide sandpaper. The JEOL JSM-6010Plus/LA analytical scanning electron microscope shown in Figure 5.4 was used in low vacuum mode to examine three specimens per cement type. Figure 5.5 displays a micrograph that was captured by detecting backscattered electrons. This image is representative of all the hardened concrete specimens that were examined. Each image revealed a complex matrix of aggregate, adhered mortar and air voids. The air voids originated from entrapping and entraining air during the mixing process and ranged in size from about 100 μm to 500 μm . Microcracks and other minor damage likely resulted from the sawing and polishing process. Otherwise, there were no signs of deterioration that would affect the mechanical behavior of the concrete.



Figure 5.4 JEOL JSM-6010Plus/LA Analytical Scanning Electron Microscope.

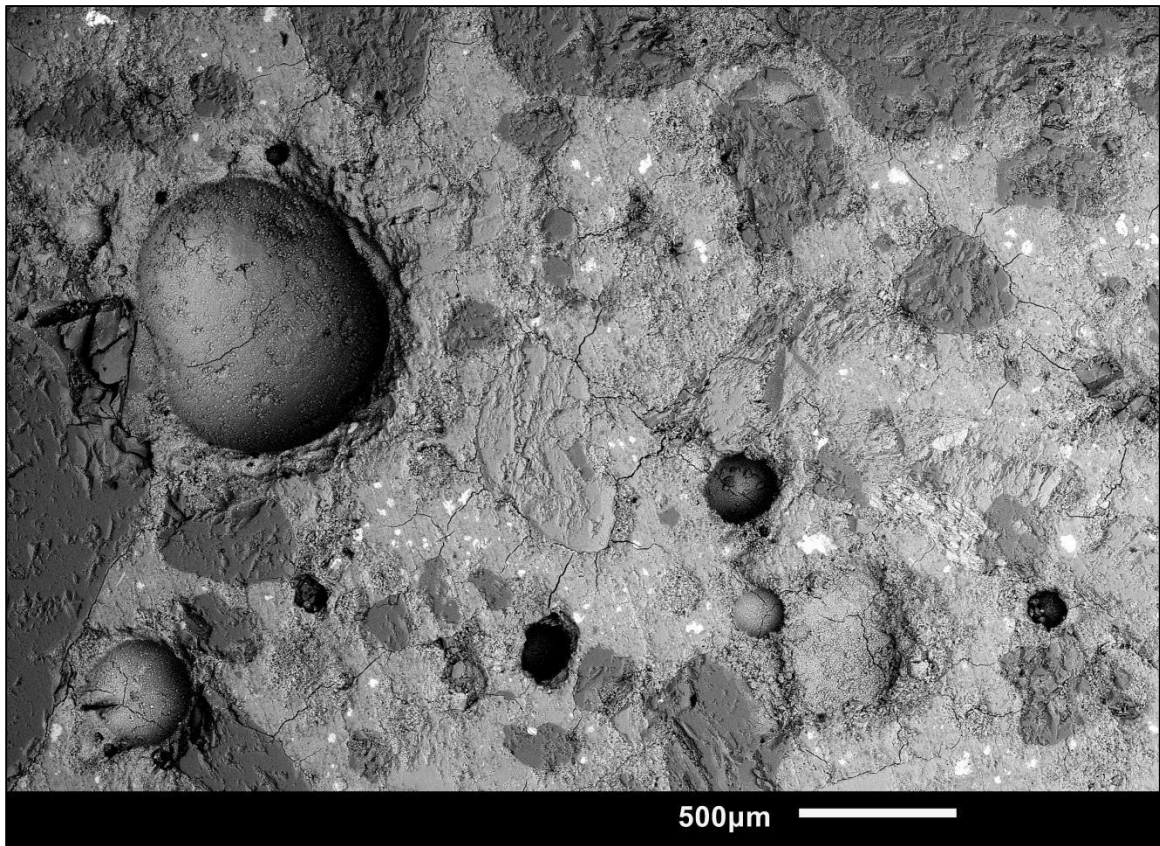


Figure 5.5 Micrograph of Concrete Matrix.

5.4 Compressive Strength

5.4.1 Background

The compressive strength of concrete is considered to be its most important characteristic. It is defined as the maximum resistance of a concrete cylinder to uniaxial loading divided by the cross sectional area of the test specimen. This mechanical property is the primary physical attribute used in the design of concrete structures. It typically ranges from 3,000 psi to 6,000 psi at 28 days for conventional concrete (Kosmatka et al., 2003).

5.4.2 Methodology and Results

Compressive strength was determined using 4×8 in. concrete cylinders in accordance with ASTM C39 (2014) at ages of 1, 3, 7, 28 and 90 days. The arrangement shown in Figure 5.6 used unbonded caps consisting of steel retainer rings with neoprene pads. For each cement type, the average compressive strength was calculated using three test specimens at each test age. As displayed in Figure 5.7, the compressive strength of concrete with Type IL(15) was comparable to Type I at 1 and 3 days. Slightly lower strengths were measured after curing for periods of 7, 28 and 90 days. Concrete based on Type IL(25) exhibited further decreases in strength throughout the measurement period as a function of its increased limestone content. With the exception of the ternary blend, all cement types were within the typical strength range for conventional concrete at 28 days. Although lower early age strength was measured for Type IT(L15)(P25) based concrete, the ternary blend had higher long term strength gain as a result of the delayed reactivity of fly ash.

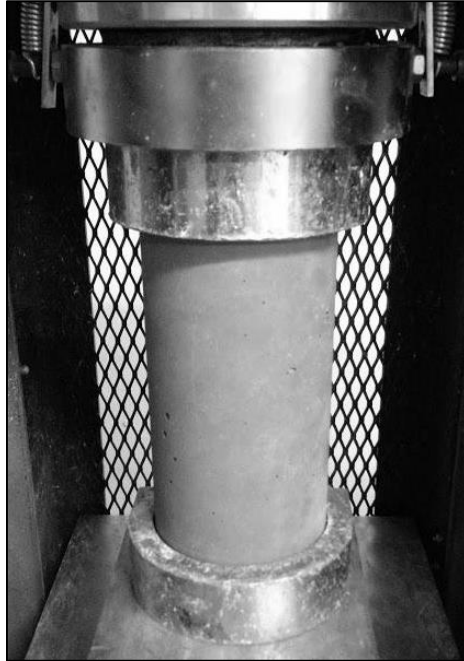


Figure 5.6 Setup for Compressing Concrete.

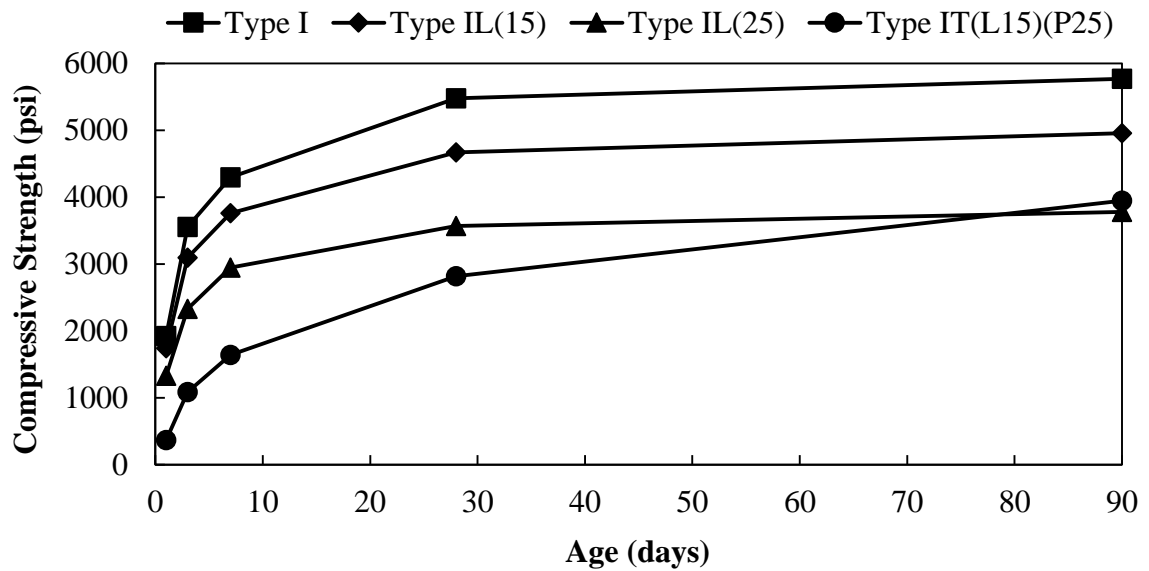


Figure 5.7 Compressive Strength of Concrete.

A linear regression analysis was performed to establish if there was a correlation between the compressive strength of the mortar and corresponding concrete throughout the testing period. Figure 5.8 shows that there was a significant correlation ($R^2 > 0.95$),

indicating that mortar strength could be used to predict the strength evolution of the companion concrete. The slope of the correlation curve for the ternary blend was found to deviate substantially from that of the other cement types. This was attributed to the standard curing procedure for mortar specimens in calcium hydroxide, whereas the concrete specimens were required to be cured in water storage tanks or a moist curing room. The calcium hydroxide reacted with the fly ash to form cementitious compounds and strengthened mortar with Type IT(L15)(P25) more rapidly than the corresponding concrete.

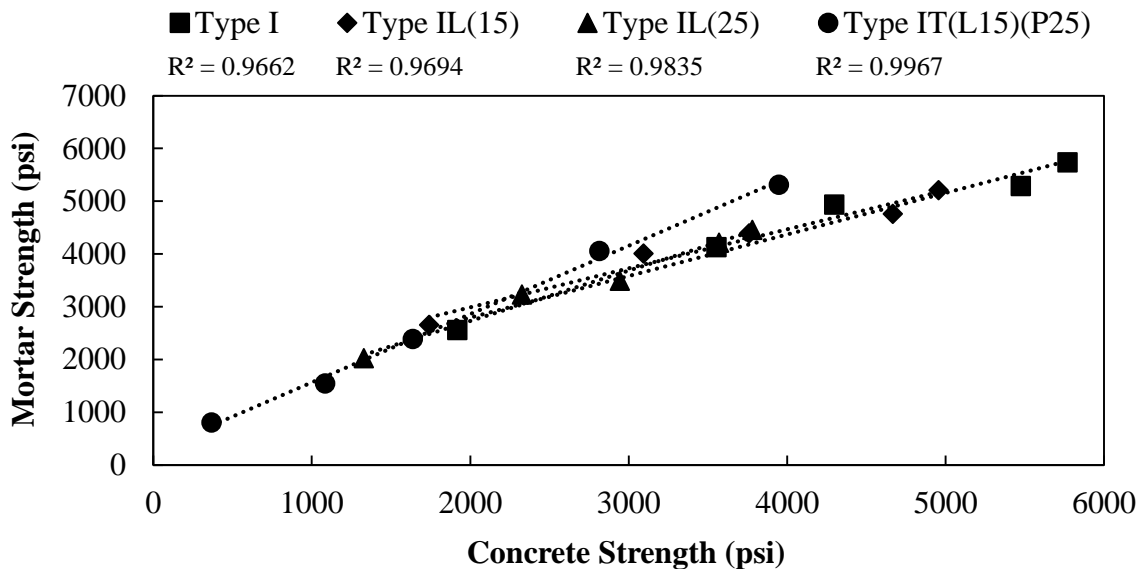


Figure 5.8 Correlation of Mortar and Concrete Compressive Strength.

5.5 Splitting Tensile Strength

5.5.1 Background

Concrete is known to have relatively high compressive strength but substantially lower tensile strength. In a study on the effect of curing, Hanson (1968) estimated the splitting tensile strength as 5 to 7.5 times the square root of the compressive strength.

This finding results in the tensile strength falling within a range of 8% to 14% of the compressive strength. The splitting tensile strength of a concrete cylinder is calculated as follows (ASTM C496, 2011):

$$T = \frac{2P}{\pi lb}$$

where:

- T = splitting tensile strength, psi
- P = maximum applied load, lbf
- l = average length, in.
- b = average diameter, in.

5.5.2 Methodology and Results

After aging for 28 days, the splitting tensile strength of 4×8 in. concrete cylinders was measured using the bearing plate and strips in the setup presented in Figure 5.9 as per ASTM C496 (2011). The average results were calculated using three specimens for each cement type.



Figure 5.9 Setup for Splitting Concrete.

The splitting tensile strengths shown in Table 5.3 ranged from 310 psi to 535 psi, decreasing with larger amounts of limestone and fly ash. On average, the splitting tensile strength was 10% of the concrete compressive strength. As per Figure 5.10, a significant correlation ($R^2 > 0.95$) was found between the splitting tensile strength and compressive strength of the concrete specimens at an age of 28 days. This finding suggested that the compressive strength could be used to estimate the tensile strength.

Table 5.3 Splitting Tensile Strength of Concrete.

Cement Type	Splitting Tensile Strength (psi)	Percentage of Compressive Strength
I	535	9.8
IL(15)	435	9.3
IL(25)	345	9.7
IT(L15)(P25)	310	11.1

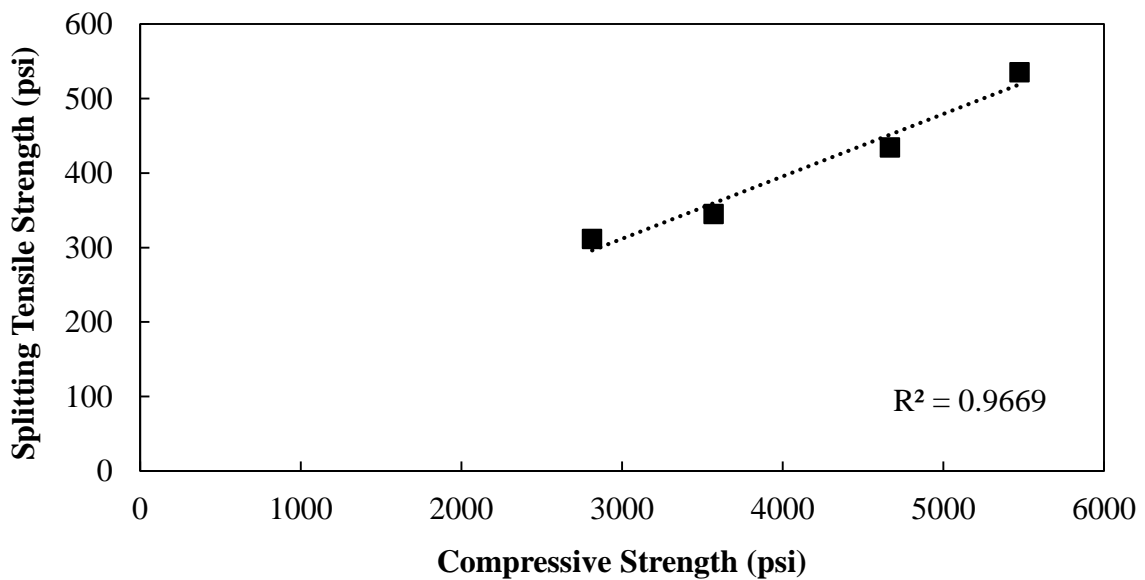


Figure 5.10 Correlation of Splitting Tensile Strength and Compressive Strength.

5.6 Flexural Strength

5.6.1 Background

Flexural strength, also referred to as modulus of rupture, is often used in the design of concrete structures and is measured using the third-point loading method with a standard concrete beam. The relationship between compressive strength and flexural strength has been well established by Wood (1992). The flexural strength of normal concrete is approximated as 7.5 to 10 times the square root of the compressive strength or about 12% to 18%. If the fracture initiates in the middle third of the span length, the modulus of rupture of a standard beam is calculated as (ASTM C78, 2010):

$$R = \frac{PL}{bd^2}$$

where:

- R = modulus of rupture, psi
- P = maximum applied load, lbf
- L = span length, in.
- b = average width at the fracture, in.
- d = average depth at the fracture, in.

5.6.2 Methodology and Results

The modulus of rupture for 6×6×20 in. concrete beams was calculated after aging 28 days by following standard test method ASTM C78 (2010) for flexural strength of concrete using third-point loading. The test setup for flexing the concrete beams is depicted in Figure 5.11, in which the supporting and loading blocks were in contact with the specimen at the third points.



Figure 5.11 Setup for Flexing Concrete.

Table 5.4 presents the average results of the flexural strength test based on using three specimens for each cement type. The modulus of rupture ranged from 505 psi to 680 psi and decreased as a consequence of intergrinding higher volumes of limestone and fly ash with the cement. The percentage of the compressive strength varied from 12.5% to 17.9% but was still within the typical range for conventional concrete. Figure 5.12 indicates that a significant correlation ($R^2 > 0.95$) was also observed between the modulus of rupture and compressive strength of concrete at 28 days.

Table 5.4 Modulus of Rupture of Concrete.

Cement Type	Modulus of Rupture (psi)	Percentage of Compressive Strength
I	680	12.5
IL(15)	640	13.7
IL(25)	570	16.0
IT(L15)(P25)	505	17.9

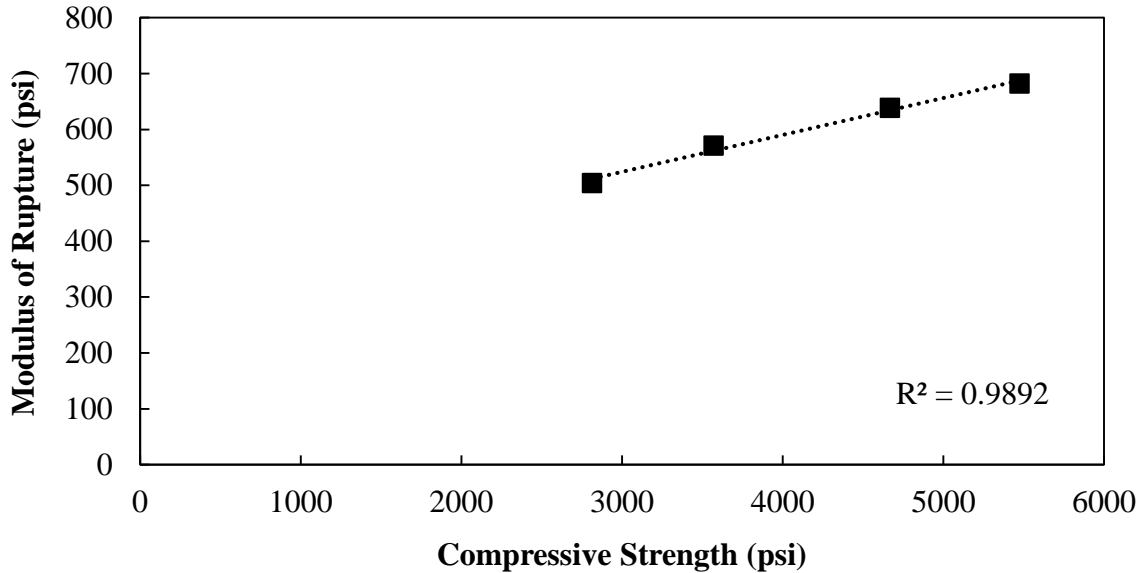


Figure 5.12 Correlation of Modulus of Rupture and Compressive Strength.

5.7 Modulus of Elasticity

5.7.1 Background

The research significance of investigating the elastic modulus is that concrete can only be utilized within its elastic range as a building material. The strain behavior of concrete in relation to an applied stress reflects its ability to deform elastically. Thus, the modulus of elasticity is defined as the slope of the stress-strain curve within a specified range. In structural design, the secant modulus is commonly used as it closely resembles the initial tangent modulus shown in Figure 5.13. The secant modulus is equal to the slope of the line from the origin to a predetermined percentage of the compressive strength (Tia et al., 2009).

Similar to the secant modulus, the chord modulus is assumed to be a straight line between specified points on the stress-strain curve. The chord modulus differs slightly by

using a starting point just above the origin as designated in ASTM C469 (2014). The following equation is used to calculate the chord modulus of elasticity:

$$E = \frac{(S_2 - S_1)}{(\varepsilon_2 - 0.000050)}$$

where:

- E = chord modulus of elasticity, psi
- S_2 = stress corresponding to 40% of the ultimate load, psi
- S_1 = stress corresponding to 50 microstrain in the longitudinal direction, psi
- ε_2 = longitudinal strain produced by S_2

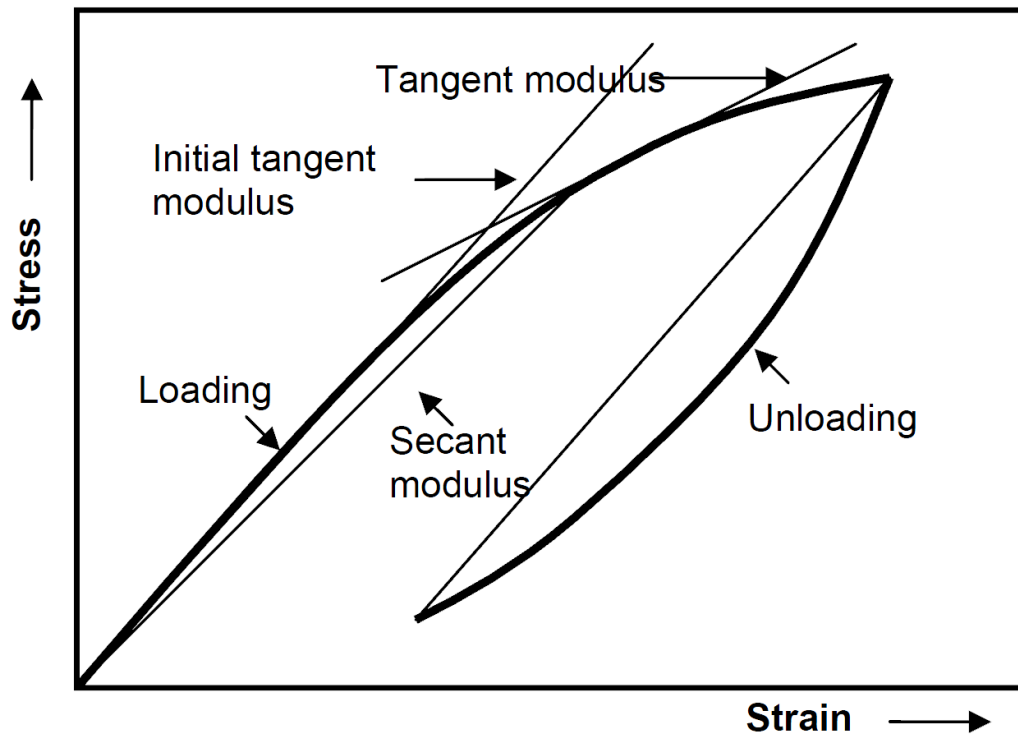


Figure 5.13 Stress-Strain Relationship of Concrete (Tia et al., 2009).

To predict the elastic modulus of concrete based on its density and compressive strength, the ACI 318 (2011) structural concrete building code recommends the use of the following model developed by Pauw (1960):

$$E = 33w_c^{1.5}\sqrt{f_c'}$$

where:

E = modulus of elasticity, psi
 w_c = density, lb/ft³
 f_c' = compressive strength, psi

Concrete is a relatively brittle material and normally has a modulus of elasticity between 2,000,000 psi and 6,000,000 psi. A comprehensive study of the performance of cement with up to 15% limestone was conducted by Barrett et al. (2013) in collaboration with the Indiana Department of Transportation. Three commercially produced Type I cements were compared to cements containing 10% to 15% interground limestone. The study concluded that there was a negligible difference in the elastic modulus of concrete as a function of limestone content.

5.7.2 Methodology and Results

A combined compressometer-extensometer with digital strain indicators was used in conjunction with a compression machine for evaluating the deformation behavior of 4×8 in. concrete cylinders at 28 days. The test setup is portrayed in Figure 5.14 with steel retainer rings and neoprene pads used to cap the cylinders. The average results of three specimens for each cement type are shown in Table 5.5 based on the procedure outlined in ASTM C469 (2014). Using the 28 day density and compressive strength, the estimated modulus of elasticity was also calculated with the ACI 318 (2011) equation for comparison. The average hardened density of 142 lb/ft³ remained fairly consistent regardless of cement type. However, the estimated modulus of elasticity decreased from 4,150,000 psi to 2,950,000 psi in relation to the corresponding compressive strengths. Whereas, the average measured modulus of elasticity was 5,100,000 psi and did not change significantly ($p > 0.05$). This comparison suggested that the ACI 318 (2011)

equation may not be a suitable prediction model for concrete based on blended cements. The results also indicated that the elastic modulus was within the normal range and that the variation was negligible when using higher volumes of limestone.



Figure 5.14 Setup for Elastically Deforming Concrete.

Table 5.5 Modulus of Elasticity of Concrete.

Cement Type	I	IL(15)	IL(25)	IT(L15)(P25)
Density (lb/ft³)	142.6	142.4	141.8	141.3
Compressive Strength (psi)	5,480	4,670	3,570	2,810
Estimated Modulus of Elasticity (psi)	4,150,000	3,850,000	3,350,000	2,950,000
Measured Modulus of Elasticity (psi)	5,500,000	5,050,000	4,850,000	5,000,000

5.8 Freeze-Thaw Resistance

5.8.1 Background

Prior to implementing blended cements with high volume interground limestone in the construction industry, it is crucial to evaluate the ability of corresponding concrete

mixtures to resist deterioration from harsh environmental conditions (TxDOT, 2013). Cold weather is one example of a potentially harmful exposure condition. In moist and cold environments, hydraulic pressure is created when water freezes and expands within the pores of the concrete matrix. Cycles of freezing and thawing can cause the cavities within concrete to rupture if the water does not have adequate space to expand or the concrete does not have sufficient strength to resist the expansion. Cracking associated with repeated cycles of freezing and thawing can substantially damage a concrete structure.

The resistance of concrete to damage from rapid freezing and thawing cycles is most commonly assessed by following the methods outlined in ASTM C215 (2014) and ASTM C666 (2015). For this test, concrete specimens are subjected to repeated cycles of freezing and thawing. Periodically, the specimens are tested for changes in mass and resonant frequency. If a specimen is able to withstand 300 freeze-thaw cycles with only limited deterioration, the concrete has high resistance to severe freeze-thaw weathering.

When a specimen is oscillated by an external force, the resonant frequency is found to be the preferential frequency at the maximum response amplitude. To measure the resonance, a forced resonance driver induces an audio frequency as per the schematic in Figure 5.15. A piezoelectric pickup converts the vibrational frequency into an electric current which is measured by a voltmeter. By forcing the test specimen to vibrate at varying frequencies, an oscilloscope is then used as a graphical display to confirm that the driver frequency at maximum signal amplitude is the resonant frequency of the specimen. After determining the frequency at which the indicator shows the maximum reading, the relative dynamic modulus of elasticity is calculated as follows:

$$P_c = \left(\frac{n_1}{n}\right)^2 \times 100$$

where:

- P_c = relative dynamic modulus of elasticity after c cycles, percent
 n_1 = fundamental transverse frequency after c cycles, Hz
 n = fundamental transverse frequency at 0 cycles, Hz

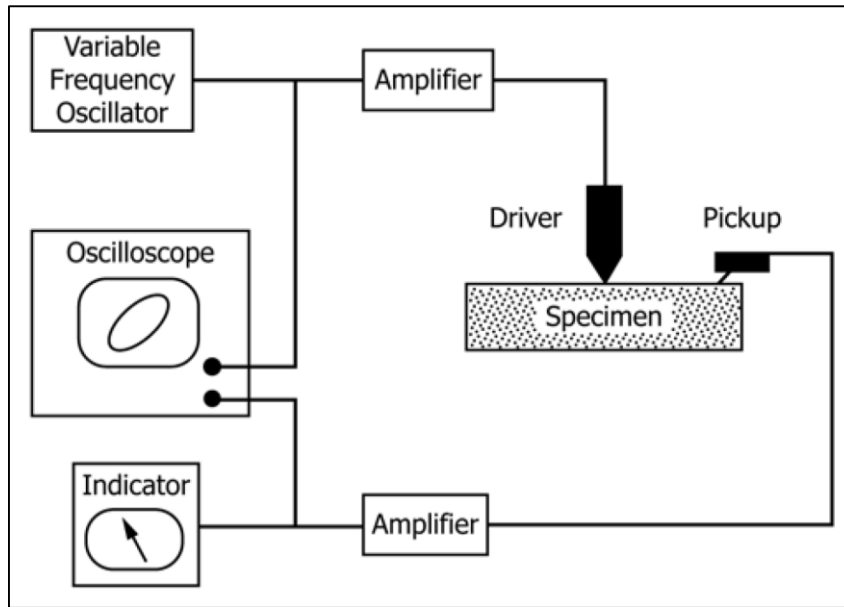


Figure 5.15 Forced Resonance Test Schematic (ASTM C215, 2014).

Concrete with a high resistance to freezing and thawing damage has a durability factor of 95 to 100. Based on the test results for the relative dynamic modulus of elasticity and the number of freeze-thaw cycles, the durability factor is calculated as:

$$DF = \frac{PN}{M}$$

where:

- DF = durability factor
 P = relative dynamic modulus of elasticity at N cycles, percent
 N = number of cycles at which P reaches a value of 60% or the number of cycles at which the exposure is to be terminated, whichever is less
 M = specified number of cycles at which the exposure is to be terminated

The freeze-thaw resistance of concrete based on portland limestone cement has primarily been investigated in Canada and Europe due to their cold climates. According to a Canadian durability study, Thomas & Hooton (2010) found no reduction in the resonant frequency of air-entrained concrete when using cement containing up to 15% limestone. Conversely, a European study by Matthews (1994) concluded that freeze-thaw resistance decreases for portland limestone cement if an air-entraining admixture is not included. Figure 5.16 serves as a guide to probable weathering severity in the United States and indicates that a moderate amount of winter precipitation and freeze-thaw cycles are expected in northern Texas according to ASTM C33 (2013). However, this study was also intended to have national relevance. Therefore, it was important to evaluate the freeze-thaw resistance of blended cements with high volume interground limestone.

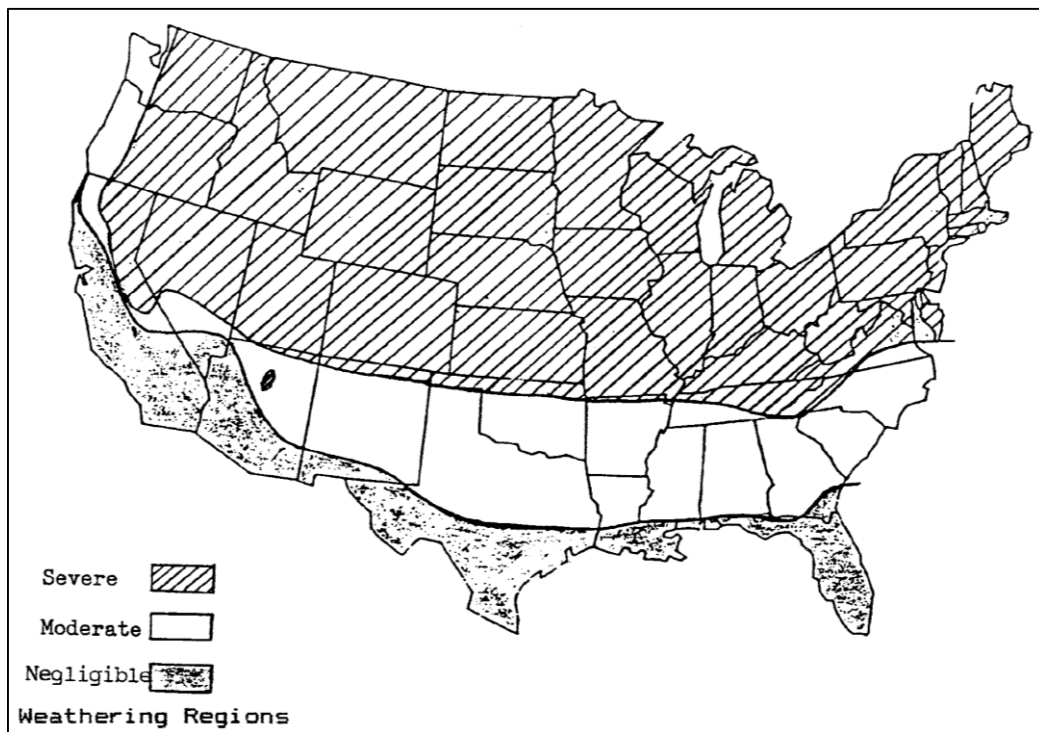


Figure 5.16 Freeze-Thaw Weathering Regions (ASTM C33, 2013).

5.8.2 Methodology and Results

To quantitatively assess the durability factor and mass change of 3×4×16 in. concrete beams, a rapid freeze-thaw cabinet was used in conjunction with a sonometer apparatus as per ASTM C666 (2015) and ASTM C215 (2014), respectively. Three specimens for each cement type were tested using the setups shown in Figures 5.17 and 5.18. The standard tests did not specify a method for calibrating the resonant frequency setup. For that reason, an aluminum calibration beam was measured prior to the concrete beams to ensure consistency of the setup throughout the testing period.



Figure 5.17 Setup for Freezing and Thawing Concrete.

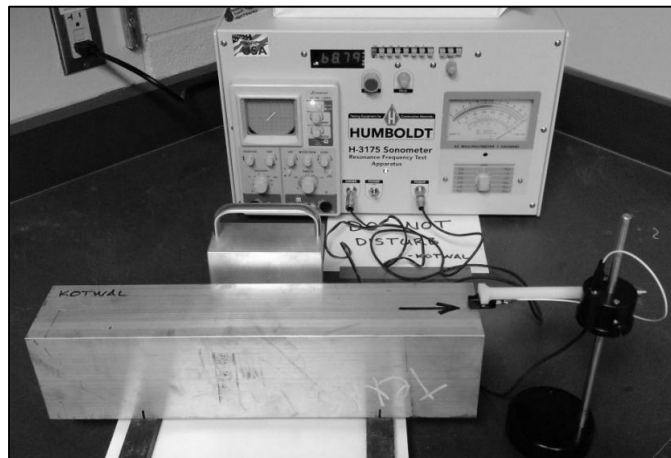


Figure 5.18 Setup for Resonating Concrete.

The average change in mass of the test specimens subjected to 300 cycles of freezing and thawing is shown in Figures 5.19 and 5.20. During the initial cycles, all concrete beams gained a small amount of mass by absorbing additional water. Subsequent cycling caused delamination of hardened cement from the surface layer of the specimens, and hydraulic pressure induced small fragments to break out of the concrete surface. With a total mass loss less than 1% after 300 freeze-thaw cycles, concrete with Type IL(15) and Type IL(25) performed similarly to Type I. Conversely, concrete based on Type IT(L15)(P25) deteriorated more rapidly and began to lose a substantial amount of mass after 150 cycles.

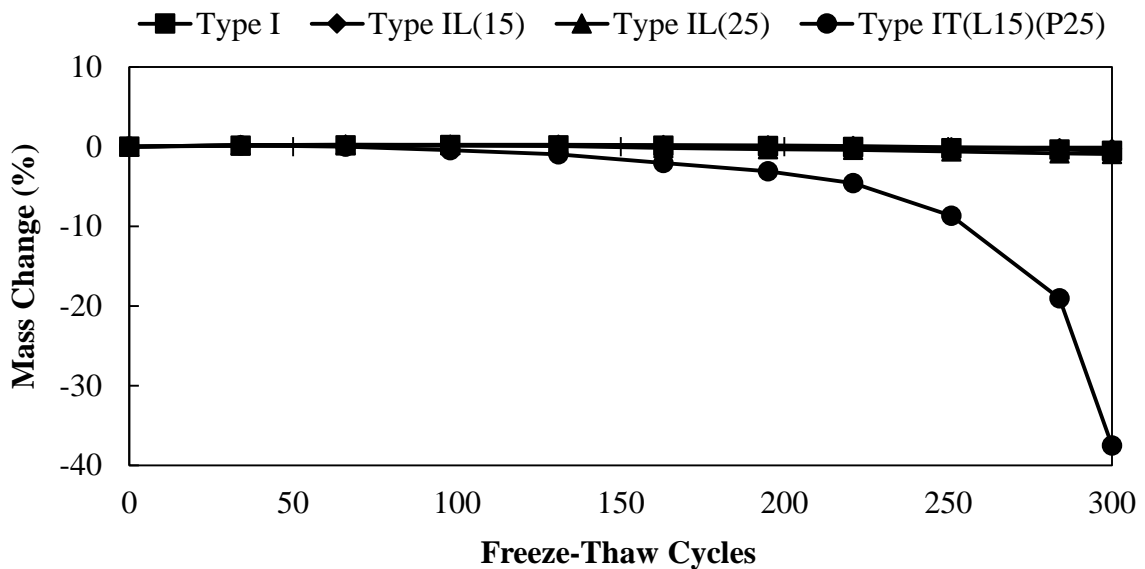
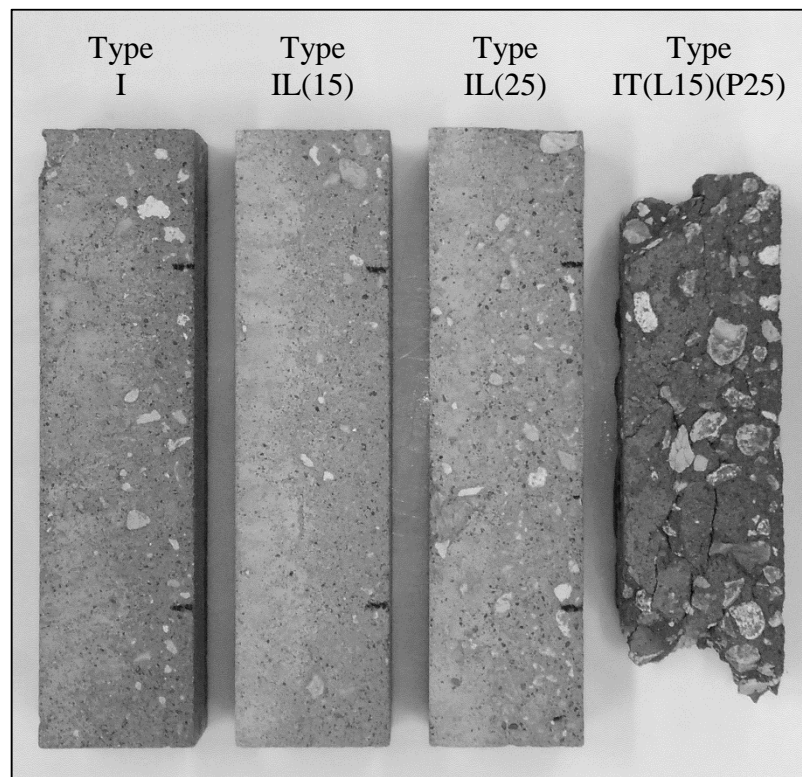


Figure 5.19 Mass Change of Concrete.

The durability factor of the concrete beams was ascertained by calculating the relative dynamic modulus of elasticity based on their initial and final fundamental transverse resonant frequencies. Table 5.6 indicates the average durability factor for each cement type and the number of cycles at which resonant frequency testing was

terminated. Durability factors greater than 95 were calculated for all cement types except the ternary blend, indicating that they have a high resistance to severe freeze-thaw weathering. The test was terminated prematurely for Type IT(L15)(P25) due to deterioration, thereby reducing its durability factor. Its underperformance likely resulted from lower early age strength, making it viable for regions with only moderate to negligible weathering conditions unless higher strength is achieved before cycling begins.



5.20 Deterioration of Concrete Beams from Freezing and Thawing.

Table 5.6 Durability Factor of Concrete.

Cement Type	Durability Factor	Test Termination (Cycles)
I	99	300
IL(15)	99	300
IL(25)	96	300
IT(L15)(P25)	78	251

VI. COMMERCIAL VIABILITY

6.1 Overview

It is estimated that in the next 10 years, the demand for cement in Texas will exceed the capacity to produce and import it. Therefore, the production of portland limestone cement presents an opportunity for cement manufacturers to increase overall production capacity (Prusinski, 2014). There is a solid foundation of limestone in Texas as indicated in Figure 6.1 by the remaining sediment of an ancient sea (TSHA, 2014). Incorporating this locally available raw material allows the amount of base cement to be reduced in concrete mixtures, thereby providing a sustainable solution for the construction industry. A cement market analysis, competitor analysis, case study review and life cycle assessment were performed to further demonstrate the commercial viability of blended cements with high volume interground limestone.

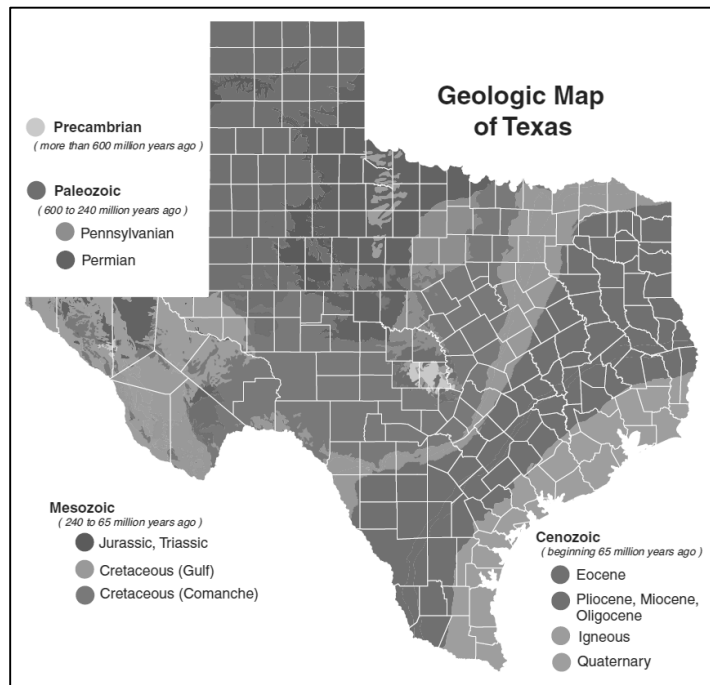


Figure 6.1 Geologic Map of Texas (TSHA, 2014).

6.2 Market Analysis

The United States cement market value is over \$7 billion, corresponding to a market volume of about 80 million tons of cement. This volume accounts for approximately 3% of global cement production and is predicted to have an annual growth of 10% (MarketLine, 2013). 48% of the cement in the United States is manufactured in five states: Texas, California, Pennsylvania, Michigan and Alabama (KEMA, 2012). Texas is the largest producer and consumer of cement in the United States with a market value over \$1 billion. As shown in Table 6.1, there are eleven manufacturing plants in Texas (CCT, 2013).

Table 6.1 Cement Plant Locations in Texas.

Company	Texas Plant Locations	Headquarters Location
Ash Grove	Midlothian	Kansas
Buzzi Unicem	Maryneal & San Antonio	Italy
Capitol Aggregates	San Antonio	Texas
Cemex	New Braunfels & Odessa	Mexico
Heidelberg	Buda & Waco	Germany
Lafarge Holcim	Midlothian	Switzerland
Martin Marietta	Midlothian & New Braunfels	North Carolina

Historically, the manufacture of portland limestone cement has been common practice in many cement plants outside of the United States. Table 6.2 indicates that cement with limestone was used in Germany during the 1960s for specialty applications before becoming an accepted product in France and Canada. Limestone was eventually permitted in cement by British standards in the 1990s, and standardization by ASTM began in the 2000s (PCA, 2010). Due to the reputable performance of portland limestone cement in Europe, it is expected that future production will continue to increase in accordance with the previous trend shown in Figure 6.2 (Hooton et al., 2007).

Table 6.2 Historical Use of Limestone in Cement (PCA, 2010).

1965	Heidelberg produces cement with 20% limestone in Germany.
1979	French standards allow limestone additions in cement.
1983	Canadian standards allow 5% limestone in Type GU cement.
1990	15% limestone used in blended cements in Germany.
1992	British standards allow up to 20% limestone in cement.
2000	European standards allow 5% limestone in all cement types.
2000	European standards create cement types with up to 35% limestone.
2004	ASTM C150 allows 5% limestone in Types I-V.
2006	Canadian standards allow 5% limestone in types other than GU.
2008	Canadian standards create cement type with up to 15% limestone.
2013	ASTM C595 allows 15% limestone in Type IL.

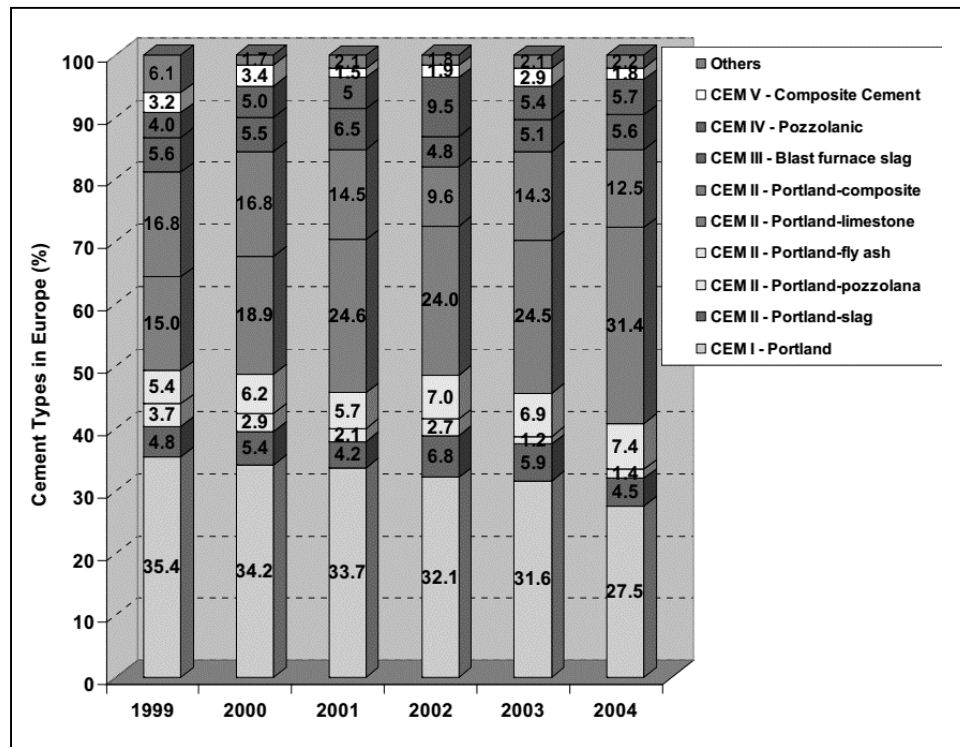


Figure 6.2 Cement Types Produced in Europe (Hooton et al., 2007).

In the recently revised standard specification for blended hydraulic cements, ASTM C595 (2013) permits Type IL to contain up to 15% limestone. The Canadian Standards Association has also adopted specifications that limit the limestone content to 15%. Yet, the use of higher amounts of limestone has been a practice in European

countries for many years. The European Committee for Standardization classifies four different types of cement containing up to 35% limestone (CEN 197, 2000). Portland limestone cement in Europe is recommended for use in reinforced concrete, precast concrete, mortars, nonstructural foundations and bound granular base layers for road construction (Cimpor, 2009).

6.3 Competitor Analysis

A limited number of cement manufacturers are producing portland limestone cement in Texas. However, the alternative of blending limestone powder with cement after production as opposed to intergrinding limestone at the plant currently presents a threat to those manufacturers. To increase value and create a performance material, limestone powder with high purity and small particle size is produced for several industrial applications. Treated calcium carbonate with a 1 μm mean particle size is sold for about \$300 per ton. This option is cost prohibitive for cement consumers, but lower grades are also sold at a reduced cost. The global market capacity for calcium carbonate is approximately 100 million tons with North America having a share of 20 million tons. The paper and polymer industries consume the largest quantity and require much higher purity limestone than the concrete industry. The major companies producing ground and precipitated calcium carbonate in North America are Omya, Imerys, Minerals Technologies, Huber, Carmeuse and Lhoist (Gauntt, 2013).

A comparison of intergrinding and blending 15% limestone with cement was conducted by Kumar et al. (2013). The research team indicated that similar performance was achieved by either intergrinding or blending. Yet, dispersion of blended limestone particles could be problematic with smaller particles and higher volumes.

6.4 Case Studies

Portland limestone cement has been used as an alternative to ordinary portland cement in many precast and ready mix applications. European cement containing up to 20% limestone was used for construction of the Gotthard Base Tunnel. Figure 6.3 presents an overview of the project site. The structure is the world's longest tunnel and passes directly under the Gotthard Mountain in Switzerland (Holcim, 2013).



Figure 6.3 Overview of the Gotthard Base Tunnel Project Site (Holcim, 2013).

Field trials of cement with 12% interground limestone were performed in Canada to construct concrete parking slabs, retaining walls, slipformed curbs and roadways. No considerable differences in performance were reported. After being weathered for several winters, there were no signs of deterioration. Thus, durability was not compromised due to the incorporation of limestone (Thomas et al., 1997). Another field trial was conducted in Ontario along King's Highway 401, the busiest highway in North America. Concrete pavement was constructed using cement containing 15% limestone, thereby reducing the carbon footprint of the project (Holcim, 2013).

Similar pavement projects have been undertaken in Colorado and Utah using concrete based on cement with 10% limestone. Specified strengths were easily achieved and the mixtures were readily constructible while also having sufficient durability and lower environmental impact. These trials demonstrated that replacing low volumes of cement with limestone can provide an adequate level of performance for civil engineering applications (Van Dam et al., 2010).

6.5 Life Cycle Assessment

6.5.1 Background

Although the performance of cement is key for its commercial viability, the importance of its environmental impact cannot be understated. A cradle-to-gate life cycle assessment of cement production involves the examination of environmental impacts by considering the energy consumed and carbon dioxide emitted during material acquisition, processing and manufacturing. This systematic analysis is used to identify and compare the positive and negative impacts of manufacturing alternative products (Williams, 2009).

A simplified process flow diagram of cement manufacturing is illustrated in Figure 6.4. Fine particulates are produced during every step of this process, resulting in the emission of aggregate and cement dust. Precautions are taken to limit the amount released into the atmosphere through the use of dust suppressors and particulate capturing devices (Huntzinger & Eatmon, 2009). Greenhouse gases are also emitted during the manufacturing process. These emissions account for 5% of global carbon dioxide production or approximately 1.7 trillion tons per year (PCA, 2007).

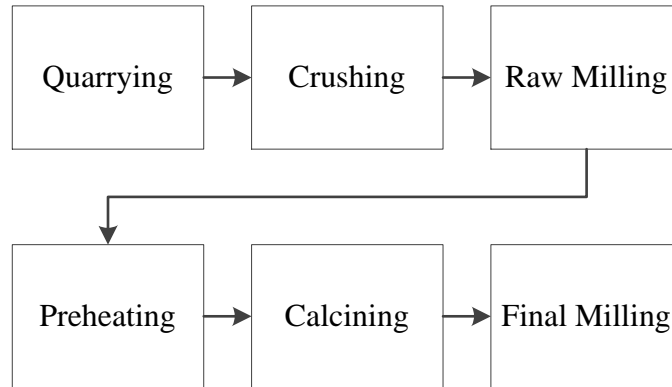


Figure 6.4 Process Flow Diagram of Cement Manufacturing.

A substantial amount of mechanical and thermal energy is required during each step of the cement manufacturing process. At a typical plant, the majority of the energy is derived from directly burning fuel, and the remainder is consumed from the electrical grid. The primary use of the energy is for the pyroprocessing of raw materials in the preheater tower and rotary kiln (Madloul et al., 2011). To supply the material on such a large scale, the cement industry in the United States consumes over 130 TWh of energy every year (Choate, 2003).

6.5.2 Methodology and Results

To evaluate the impact of blended cements on production volume, energy consumption and carbon dioxide emissions, an inventory of data was first collected from a life cycle assessment study published by Choate (2003) for the United States Department of Energy. Supplementary information was also obtained from the Office of Resource Conservation and Recovery (EPA, 2010). The energy consumption and carbon dioxide emissions per ton of Type I cement from an average manufacturing process were separated into the four steps shown in Table 6.3. Values for transporting and conveying material were accounted for in the process steps.

Table 6.3 Energy Consumption and CO₂ Emissions of Cement Manufacturing.

Process Step	Energy Consumption (kWh/ton)	CO₂ Emissions (ton/ton)
Quarrying & Crushing	11.4	0.004
Raw Milling	24.9	0.017
Preheating & Calcining	1,226.2	0.976
Final Milling	71.9	0.049
Total for Type I Cement	1,334.4	1.046

Based on the inventory of data, values were adjusted to simulate changes due to the incorporation of limestone and fly ash in the final milling step. The cement plant must have excess grinding capacity compared to clinker production to increase production volume, and it was assumed that the final milling duration remained constant. The plant must also have sufficient storage capacity for the final product.

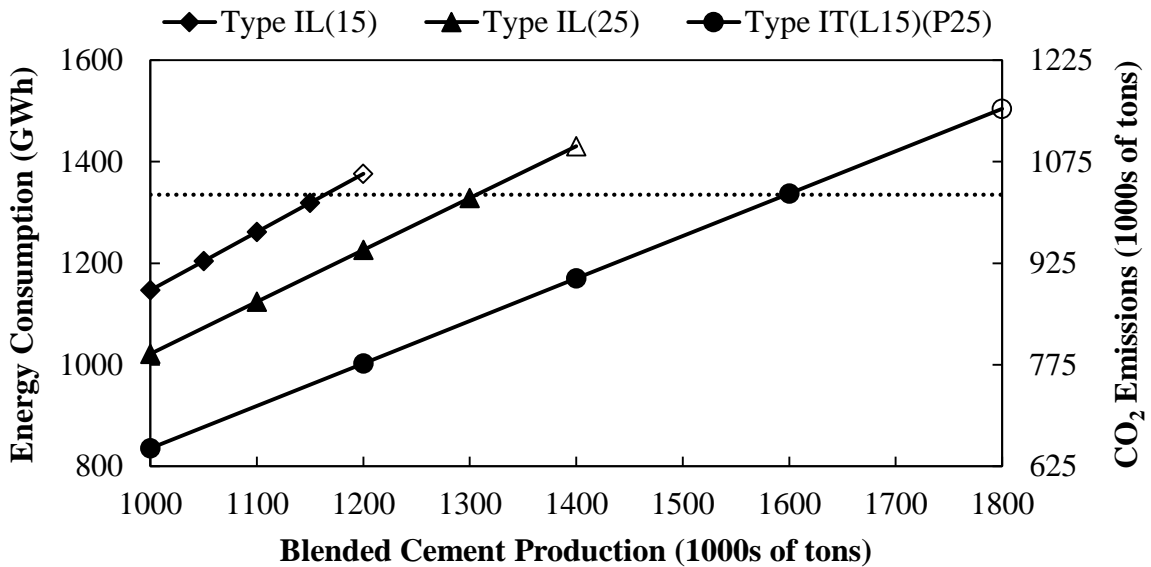
The effect of producing blended cements on energy and emissions is presented in Table 6.4 using nominal values of limestone and fly ash. The results of the analysis indicated that less energy was consumed and less carbon dioxide was emitted per ton of blended cement as the amount of interground limestone and fly ash increased.

Table 6.4 Energy Consumption and CO₂ Emissions of Blended Cement Manufacturing.

Cement Type	Energy Consumption (kWh/ton)	CO₂ Emissions (ton/ton)
I	1,334.4	1.046
IL(15)	1,146.7	0.896
IL(25)	1,021.6	0.797
IT(L15)(P25)	835.6	0.650

Further analysis was conducted for the life cycle assessment to establish whether a larger amount of blended cement could be produced without exceeding the energy and emissions resulting from the conventional manufacturing process. A breakeven point

was established based on a cement plant that produces 1 million tons of Type I cement per year. This point is shown as a dotted line in Figure 6.5. As the cement plant converted to produce an equivalent amount of one of the blended cement types, then the energy and emissions substantially decreased. Additionally, the plant was able to increase blended cement production while remaining below the breakeven point. Without exceeding the manufacturing capability of the cement plant, the production of Type IL(15), Type IL(25) and Type IT(L15)(P25) reached the breakeven point at approximately 1.15 million, 1.3 million and 1.6 million tons, respectively. Data points with no fill are theoretical, as the capacity of the plant was exceeded in terms of production volume, energy consumption and carbon dioxide emissions.



* Data points with no fill are theoretical.
 ** Dotted line represents breakeven point.

Figure 6.5 Energy Consumption and CO₂ Emissions of Blended Cement Manufacturing.

VII. DISCUSSION

7.1 Summary

An experimental program was conducted to evaluate the effect of high volume interground limestone on the characteristics of blended cements as well as the properties of mortar and concrete manufactured with the blended cements. Results from this study indicate that the blended cements can be used as an alternative to ordinary cement. Based on the established parameters, concentrations of interground limestone up to 25% are acceptable. However, the use of cement in combination with limestone and Class F fly ash does present some issues, the most serious being lower early age strength and reduced freeze-thaw resistance of concrete produced with such blended cement.

7.2 Conclusions

The following conclusions were drawn from the results of this study:

- The surface area of the cement increased as higher volumes of limestone and fly ash were interground with clinker. A particle size distribution analysis indicated that the increased surface area resulted from a larger volume percentage of fine particulates.
- The concentration of the primary cement phases decreased as a function of incorporating the mineral admixtures. Consequently, less energy was produced during hydration of the blended cements, resulting in delayed setting time and lower early age strength compared to ordinary cement.
- Mortar based on Type IL(15) and Type IL(25) fulfilled the strength requirements specified in ASTM C595 (2013) and ASTM C1157 (2011), respectively.

Although mortar with Type IT(L15)(P25) did not meet the specification at 3 and 7 days, its strength increased by 28 days to fulfill the physical requirement.

- There was a significant correlation between the compressive strength of the mortar and corresponding concrete throughout the testing period. Thus, the mortar strength could be used to predict the strength evolution of the companion concrete.
- The compressive strength of concrete with Type IL(15) was comparable to Type I at 1 and 3 days. Slightly lower strengths were measured after 7, 28 and 90 days. Concrete based on Type IL(25) exhibited further decreases in strength throughout the 90 day test period due to its higher limestone content. Although even lower early age strength was measured for Type IT(L15)(P25) based concrete, the ternary blend had higher long term strength gain as a result of the delayed formation of fly ash hydration products.
- There was a significant correlation between the compressive strength of the concrete and corresponding tensile and flexural strength at 28 days. This finding indicated that the compressive strength could be used to estimate the tensile and flexural strength.
- The measured modulus of elasticity of concrete did not change significantly, as the variation due to the effect of cement type was negligible. A comparison between the measured and estimated elastic modulus resulted in the conclusion that the ACI 318 (2011) equation may not be a suitable prediction model for concretes based on blended cements.

- Compared to ordinary cement, a slight reduction in long term drying shrinkage was measured for the blended cements. The main effect of cement type on drying shrinkage was statistically significant at 90 days. A reduction in length change corresponds with improved volumetric stability and lower potential for cracking.
- Durability factors greater than 95 were calculated for all cement types except the ternary blend, indicating that they have a high resistance to severe freeze-thaw weathering. With only a minor loss in mass from hydraulic pressure, concrete with Type IL(15) and Type IL(25) performed similarly to Type I. Conversely, concrete based on Type IT(L15)(P25) deteriorated rapidly, losing a substantial amount of mass. Its underperformance likely resulted from lower early age strength, making it viable for regions with only moderate to negligible weathering conditions unless higher strength is achieved before freeze-thaw cycling begins.
- The life cycle assessment of cement production indicated that less energy was consumed and less carbon dioxide was emitted per ton of blended cement as the amount of interground limestone and fly ash increased. Further analysis concluded that production volume increased without exceeding the energy and emissions resulting from the conventional manufacturing process.

7.3 Recommendations

Based on the conclusions, the following recommendations were made:

- To increase strength of the blended cements, constructors may be required to use concrete mixtures with a lower water-cement ratio. If the fresh concrete mixtures are too stiff, plasticizers are recommended for improving the workability.

- Another option for improving performance is for the manufacturer to grind the blended cements for a longer duration in the finish mill to increase fineness, although this would reduce output and increase energy and emissions.
- Cement with high volume interground limestone has sufficient freeze-thaw resistance for use in severe weathering regions. Winter conditions may limit construction with Type IT(L15)(P25) as a result of its extended setting time and slow strength gain. A longer curing period is recommended before freezing begins to allow the concrete to achieve higher strength.
- The blended cements would be beneficial in precast applications due to the demand for high volumes of cement in self consolidating concrete. Setting time could be reduced by altering the mixture to allow for faster turnover of formwork and hasten the point at which the concrete can bear a load. Other recommended applications include flatwork, such as pavements, foundations, driveways and sidewalks.

7.4 Future Research

Additional research is needed to support the commercialization of blended cements with high volume interground limestone. Future studies should investigate the following topics:

- Field trials of blended cements with high volume interground limestone.
- Properties of blended cements with varying water-cement ratios.
- The effect of grinding duration on the performance of blended cements.
- Ternary blended cement with limestone and Class C fly ash.
- Cost analysis and material depletion assessment of blended cement production.

LITERATURE CITED

- ACI 318. (2011). *Building code requirements for structural concrete*. Farmington Hills, Michigan: American Concrete Institute.
- ACI CP1. (2015). *Concrete field testing technician - Grade I*. Farmington Hills, Michigan: American Concrete Institute.
- ACI E701. (2007). *Aggregates for concrete*. Farmington Hills, Michigan: American Concrete Institute.
- ASTM C1012. (2013). *Standard test method for length change of hydraulic cement mortars exposed to a sulfate solution*. West Conshohocken, Pennsylvania: ASTM International.
- ASTM C1064. (2012). *Standard test method for temperature of freshly mixed hydraulic cement concrete*. West Conshohocken, Pennsylvania: ASTM International.
- ASTM C109. (2013). *Standard test method for compressive strength of hydraulic cement mortars*. West Conshohocken, Pennsylvania: ASTM International.
- ASTM C1157. (2011). *Standard performance specification for hydraulic cement*. West Conshohocken, Pennsylvania: ASTM International.
- ASTM C127. (2012). *Standard test method for density, relative density and absorption of coarse aggregate*. West Conshohocken, Pennsylvania: ASTM International.
- ASTM C128. (2012). *Standard test method for density, relative density and absorption of fine aggregate*. West Conshohocken, Pennsylvania: ASTM International.
- ASTM C136. (2006). *Standard test method for sieve analysis of fine and coarse aggregates*. West Conshohocken, Pennsylvania: ASTM International.

- ASTM C138. (2014). *Standard test method for density (unit weight), yield and air content (gravimetric) of concrete*. West Conshohocken, Pennsylvania: ASTM International.
- ASTM C143. (2012). *Standard test method for slump of hydraulic cement concrete*. West Conshohocken, Pennsylvania: ASTM International.
- ASTM C1437. (2013). *Standard test method for flow of hydraulic cement mortar*. West Conshohocken, Pennsylvania: ASTM International.
- ASTM C150. (2012). *Standard specification for portland cement*. West Conshohocken, Pennsylvania: ASTM International.
- ASTM C192. (2014). *Standard practice for making and curing concrete test specimens in the laboratory*. West Conshohocken, Pennsylvania: ASTM International.
- ASTM C204. (2011). *Standard test methods for fineness of hydraulic cement by air permeability apparatus*. West Conshohocken, Pennsylvania: ASTM International.
- ASTM C215. (2014). *Standard test method for fundamental transverse, longitudinal and torsional resonant frequencies of concrete specimens*. West Conshohocken, Pennsylvania: ASTM International.
- ASTM C231. (2014). *Standard test method for air content of freshly mixed concrete by the pressure method*. West Conshohocken, Pennsylvania: ASTM International.
- ASTM C305. (2014). *Standard practice for mechanical mixing of hydraulic cement pastes and mortars of plastic consistency*. West Conshohocken, Pennsylvania: ASTM International.
- ASTM C33. (2013). *Standard specification for concrete aggregates*. West Conshohocken, Pennsylvania: ASTM International.

ASTM C39. (2014). *Standard test method for compressive strength of cylindrical concrete specimens*. West Conshohocken, Pennsylvania: ASTM International.

ASTM C403. (2008). *Standard test method for time of setting of concrete mixtures by penetration resistance*. West Conshohocken, Pennsylvania: ASTM International.

ASTM C469. (2014). *Standard test method for static modulus of elasticity and Poisson's ratio of concrete in compression*. West Conshohocken, Pennsylvania: ASTM International.

ASTM C496. (2011). *Standard test method for splitting tensile strength of cylindrical concrete specimens*. West Conshohocken, Pennsylvania: ASTM International.

ASTM C566. (2013). *Standard test method for total evaporable moisture content of aggregate by drying*. West Conshohocken, Pennsylvania: ASTM International.

ASTM C595. (2013). *Standard specification for blended hydraulic cements*. West Conshohocken, Pennsylvania: ASTM International.

ASTM C596. (2009). *Standard test method for drying shrinkage of mortar containing hydraulic cement*. West Conshohocken, Pennsylvania: ASTM International.

ASTM C666. (2015). *Standard test method for resistance of concrete to rapid freezing and thawing*. West Conshohocken, Pennsylvania: ASTM International.

ASTM C778. (2013). *Standard specification for standard sand*. West Conshohocken, Pennsylvania: ASTM International.

ASTM C78. (2010). *Standard test method for flexural strength of concrete using simple beam with third-point loading*. West Conshohocken, Pennsylvania: ASTM International.

- ASTM D75. (2014). *Standard practice for sampling aggregates*. West Conshohocken, Pennsylvania: ASTM International.
- Atakan, V., Jain, J., Ravikumar, D., McCandlish, L., & DeCristofaro, N. (2014). *Water savings in concrete made from solidia cement*. Piscataway, New Jersey: Solidia Technologies.
- Barrett, T. J., Sun, H., & Weiss, W. J. (2013). *Performance of portland limestone cements: Cements designed to be more sustainable that include up to 15% limestone addition*. West Lafayette, Indiana: Indiana Department of Transportation.
- Brookbanks, P. (1993). *Performance of limestone filled cements*. Watford, United Kingdom: Building Research Establishment.
- Caldarone, M. A. (2006). *Effect of use of limestone on various properties of portland cement*. Skokie, Illinois: Portland Cement Association.
- Callister, W. D., & Rethwisch, D. G. (2010). *Materials science and engineering: An introduction*. Hoboken, New Jersey: John Wiley & Sons.
- CCAA. (2002). *Drying shrinkage of cement and concrete*. Sydney, Australia: Cement, Concrete and Aggregates Australia.
- CCT. (2013). *Texas cement industry: Vital for Texas' future*. Hurst, Texas: Cement Council of Texas.
- CEN 197. (2000). *Composition, specifications and conformity criteria for common cements*. Brussels, Belgium: European Committee for Standardization.
- Choate, W. T. (2003). *Energy and emission reduction opportunities for the cement industry*. Washington, District of Columbia: United States Department of Energy.

- Cimpor. (2009). *Portland limestone cement CEM II/B-L*. Lisbon, Portugal: Cimpor.
- Civil Engineers Forum. (2015). *The role of aggregate in concrete mixes*. Retrieved from
Civil Engineers Forum: www.civilengineersforum.com
- Copeland, L. E., Kantro, D. L., & Verbeck, G. (1960). *Chemistry of hydration of portland cement*. Skokie, Illinois: Portland Cement Association.
- Crammond, N. (2003). The thaumasite form of sulfate attack in the United Kingdom.
Cement and Concrete Composites, 25, 809-818.
- Detwiler, R. J. (1995). *Effects on cement of high efficiency separators*. Skokie, Illinois:
Portland Cement Association.
- Detwiler, R. J. (1996). *Properties of concretes made with fly ash and cements containing limestone*. Skokie, Illinois: Portland Cement Association.
- Detwiler, R. J., Bhatti, J. I., & Bhattacharja, S. (1996). *Supplementary cementing materials for use in blended cements*. Skokie, Illinois: Portland Cement Association.
- Drimalas, T., Clement, J. C., Folliard, K. J., Dhole, R., & Thomas, M. D. (2011).
Laboratory and field evaluations of external sulfate attack in concrete. Austin, Texas: Texas Department of Transportation.
- EPA. (2010). *Waste reduction model: Fly ash*. Washington, District of Columbia: United States Environmental Protection Agency.
- Gauntt, J. (2013). *Ground calcium carbonate*. Englewood, Colorado: Mining Engineering.

- Goldstein, J., Newbury, D. E., Joy, D. C., Lyman, C. E., Echlin, P., Lifshin, E., . . .
Michael, J. R. (2012). *Scanning electron microscopy and X-ray microanalysis*.
New York, New York: Springer Science & Business Media.
- Hanson, J. A. (1968). *Effects of curing and drying environments on splitting tensile strength of concrete*. Skokie, Illinois: Portland Cement Association.
- Hawkins, P., Tennis, P., & Detwiler, R. (2003). *The use of limestone in portland cement: A state of the art review*. Skokie, Illinois: Portland Cement Association.
- Hill, R. L., & Folliard, K. J. (2006). *The impact of fly ash on air-entrained concrete*.
Silver Spring, Maryland: National Ready Mixed Concrete Association.
- Holcim. (2013). *The Gotthard base tunnel: An innovative journey to a world record*.
Jona, Switzerland: Holcim.
- Hooton, R. D. (1990). *Effects of carbonate additions on heat of hydration and sulfate resistance of portland cement*. West Conshohocken, Pennsylvania: ASTM International.
- Hooton, R. D., & Thomas, M. D. (2002). *The use of limestone in portland cements: Effect on thaumasite form of sulfate attack*. Skokie, Illinois: Portland Cement Association.
- Hooton, R. D., Nokken, M., & Thomas, M. D. (2007). *Portland limestone cement: State of the art report and gap analysis*. Ottawa, Ontario: Cement Association of Canada.
- Huntzinger, D. N., & Eatmon, T. D. (2009). A life cycle assessment of portland cement manufacturing: Comparing the traditional process with alternative technologies. *Journal of Cleaner Production*, 17, 668-675.

- KEMA. (2012). *Industrial sectors market characterization*. Arnhem, Netherlands: Keuring van Elektrotechnische Materialen te Arnhem.
- Kosmatka, S. H., Kerkhoff, B., & Panarese, W. C. (2003). *Design and control of concrete mixtures*. Skokie, Illinois: Portland Cement Association.
- Kotwal, A. R., Kim, Y. J., Hu, J., & Sriraman, V. (2014). Characterization and early age physical properties of ambient cured geopolymer mortar based on Class C fly ash. *International Journal of Concrete Structures and Materials*, 9, 35-43.
- Kumar, A., Oey, T., Falla, G. P., Henkensiefken, R., Neithalath, N., & Sant, G. (2013). A comparison of intergrinding and blending limestone on reaction and strength evolution in cementitious materials. *Construction and Building Materials*, 43, 428-435.
- Leng, Y. (2008). *Materials characterization: Introduction to microscopic and spectroscopic methods*. Singapore: John Wiley & Sons.
- Livesey, P. (1991). Performance of limestone filled cements. *Blended Cements in Construction*, 1-15.
- Madlool, N. A., Saidur, R., Hossain, M. S., & Rahim, N. A. (2011). A critical review on energy use and savings in the cement industries. *Renewable and Sustainable Energy Reviews*, 15, 2042-2060.
- Malvern. (2015). *Laser diffraction*. Worcestershire, United Kingdom: Malvern Instruments.
- MarketLine. (2013). *Cement in the United States*. London, United Kingdom: Informa Business.

- Matthews, J. D. (1994). Performance of limestone filler cement concrete. *Euro-Cements*, 113-147.
- Neville, A. M. (2006). *Concrete: Neville's insights and issues*. London, United Kingdom: Thomas Telford.
- Pauw, A. (1960). *Static modulus of elasticity of concrete as affected by density*. Farmington Hills, Michigan: American Concrete Institute.
- PCA. (2007). *Green in practice: Concrete, cement and carbon dioxide*. Skokie, Illinois: Portland Cement Association.
- PCA. (2010). *Portland limestone blended cement in AASHTO M240 and ASTM C595*. Skokie, Illinois: Portland Cement Association.
- Powers, T. C. (1948). *A discussion of cement hydration in relation to the curing of concrete*. Skokie, Illinois: Portland Cement Association.
- Prusinski, J. R. (2014). Texas cement demand presents challenges, opportunities. *TACA Conveyor, Winter*, 16-19.
- RRUFF. (2015). *Calcite*. Retrieved from RRUFF: www.ruff.info
- Santhanam, M., Cohen, M. D., & Olek, J. (2001). Sulfate attack research: Whither now. *Cement and Concrete Research*, 845-851.
- Schiller, B., & Ellerbrock, H. G. (1992). The grinding and properties of cement with several main constituents. *Zement-Kalk-Gips*, 45 (7), 325-334.
- Schmidt, M. (1992). Cement with interground additives: Capabilities and environmental relief. *Zement-Kalk-Gips*, 45 (2), 64-69.
- Schmidt, M., Harr, K., & Boeing, R. (1993). Blended cement according to ENV 197 and experiences in Germany. *Cement, Concrete and Aggregates*, 15 (2), 156-164.

- Schmidt, M., Middendorf, B., Vellmer, C., & Geisenhanslueke, C. (2004). *Innovations in portland cement manufacturing*. Skokie, Illinois: Portland Cement Association.
- Seto, K. C., Guneralp, B., & Hutyra, L. R. (2012). Global forecasts of urban expansion to 2030 and direct impacts on biodiversity and carbon pools. In B. L. Turner (Ed.), *Proceedings of the National Academy of Sciences of the United States of America*, 109, pp. 16083-16088. Boston, Massachusetts: Yale University.
- Smith, F. (1999). *Industrial applications of X-ray diffraction*. New York, New York: Marcel Dekker.
- Sprung, S., & Siebel, E. (1991). Assessment of the suitability of limestone for producing portland limestone cement. *Zement-Kalk-Gips*, 44 (1), 1-11.
- Tanesi, J., Bentz, D., & Ardani, A. (2013). *Enhancing the performance of high volume fly ash concretes using fine limestone powder*. McLean, Virginia: Federal Highway Administration.
- Tang, F. J. (1992). *Optimization of sulfate form and content*. Skokie, Illinois: Portland Cement Association.
- Taylor, H. F. (1997). *Cement chemistry*. London, United Kingdom: Thomas Telford.
- Tennis, P. D., Thomas, M. D., & Weiss, W. J. (2011). *State of the art report on use of limestone in cements at levels of up to 15%*. Skokie, Illinois: Portland Cement Association.
- Thomas, J., & Jennings, H. (2015). *The science of concrete*. Evanston, Illinois: Northwestern University.
- Thomas, M. D., & Hooton, R. D. (2010). *The durability of concrete produced with portland limestone cement*. Skokie, Illinois: Portland Cement Association.

- Thomas, M. D., Cail, K., Blair, B., Delagrave, A., Masson, P., & Kazanis, K. (1997). Use of low CO₂ portland limestone cement for pavement construction in Canada. *International Journal of Pavement Research Technology*, 3 (5), 228-233.
- Tia, M., Liu, Y., Haranki, B., & Su, Y. M. (2009). *Modulus of elasticity, creep and shrinkage of concrete - Phase II*. Gainesville, Florida: University of Florida.
- TSHA. (2014). *Geology of Texas*. Denton, Texas: Texas State Historical Association.
- TxDOT. (2013). *Evaluating limestone cements containing greater than 15% limestone*. Austin, Texas: Texas Department of Transportation.
- Van Dam, T., Smartz, B., & Laker, T. (2010). Performance enhancing research shows ways of reducing concrete's footprint. *Roads and Bridges*.
- WBCSD. (2012). *Cement sustainability initiative*. Geneva, Switzerland: World Business Council for Sustainable Development.
- Whiting, D. A., & Nagi, M. A. (1998). *Manual on the control of air content in concrete*. Skokie, Illinois: Portland Cement Association.
- Williams, A. S. (2009). *Life cycle analysis: A step by step approach*. Champaign, Illinois: Illinois Sustainable Technology Center.
- Wood, S. L. (1992). *Evaluation of the long term properties of concrete*. Skokie, Illinois: Portland Cement Association.